NEOPLASIA
www.neoplasia.com

Volume 20 Number 3 March 2018 pp. 263–279 263

BAG3 Overexpression and Cytoprotective Autophagy Mediate Apoptosis Resistance in Chemoresistant Breast Cancer Cells

Chandan Kanta Das[*,#], Benedikt Linder[*], Florian Bonn[†], Florian Rothweiler[‡], Ivan Dikic[†,§], Martin Michaelis[‡,¶], Jindrich Cinatl[‡], Mahitosh Mandal[#] and Donat Kögel[*,]**

*Experimental Neurosurgery, Neuroscience Center, Goethe University Hospital, Frankfurt am Main, Germany; [†]Institute of Biochemistry II, Goethe University Hospital, Frankfurt am Main, Germany; [‡]Institute for Medical Virology, Goethe University Hospital, Frankfurt am Main, Germany; [§]Buchmann Institute for Molecular Life Sciences, Goethe University, Frankfurt am Main, Germany; [¶]School of Biosciences, The University of Kent, Canterbury, Kent, UK; [#]School of Medical Science and Technology, Indian Institute of Technology Kharagpur, Kharagpur, West Bengal, India; [**]German Cancer Consortium (DKTK), Germany

Abstract

Target-specific treatment modalities are currently not available for triple-negative breast cancer (TNBC), and acquired chemotherapy resistance is a primary obstacle for the treatment of these tumors. Here we employed derivatives of BT-549 and MDA-MB-468 TNBC cell lines that were adapted to grow in the presence of either 5-Fluorouracil, Doxorubicin or Docetaxel in an aim to identify molecular pathways involved in the adaptation to drug-induced cell killing. All six drug-adapted BT-549 and MDA-MB-468 cell lines displayed cross resistance to chemotherapy and decreased apoptosis sensitivity. Expression of the anti-apoptotic co-chaperone BAG3 was notably enhanced in two thirds (4/6) of the six resistant lines simultaneously with higher expression of HSP70 in comparison to parental controls. Doxorubicin-resistant BT-549 (BT-549^{r}DOX^{20}) and 5-Fluorouracil-resistant MDA-MB-468 (MDA-MB-468^{r}5-FU^{2000}) cells were chosen for further analysis with the autophagy inhibitor Bafilomycin A1 and lentiviral depletion of ATG5, indicating that enhanced cytoprotective autophagy partially contributes to increased drug resistance and cell survival. Stable lentiviral BAG3 depletion was associated with a robust down-regulation of Mcl-1, Bcl-2 and Bcl-xL, restoration of drug-induced apoptosis and reduced cell adhesion in these cells, and these death-sensitizing effects could be mimicked with the BAG3/Hsp70 interaction inhibitor YM-1 and by KRIBB11, a selective transcriptional inhibitor of HSF-1. Furthermore, BAG3 depletion was able to revert the EMT-like transcriptional changes observed in BT-549^{r}DOX^{20} and MDA-MB-468^{r}5-FU^{2000} cells. In summary, genetic and pharmacological interference with BAG3 is capable to resensitize TNBC cells to treatment, underscoring its relevance for cell death resistance and as a target to overcome therapy resistance of breast cancer.

Neoplasia (2018) 20, 263–279

Abbreviations: TNBC, Triple negative breast cancer; DOX, Doxorubicin; DOC, Docetaxel; 5-FU, 5-Fluorouracil; Baf A1, Bafilomycin A1; STS, Staurosporine; BAG3, Bcl-2-associated athanogene 3; HSP70, Heat shock protein 70; HSF1, Heat shock factor 1; Par, Parental; Ctrl, Control; KD, Knockdown

Address all correspondence to: Donat Kögel, Experimental Neurosurgery, Neuroscience Center, Theodor-Stern-Kai 7, Goethe University Hospital, D-60590 Frankfurt am Main.
E-mail: koegel@em.uni-frankfurt.de

Received 4 October 2017; Revised 22 December 2017; Accepted 3 January 2018

1476-5586
https://doi.org/10.1016/j.neo.2018.01.001

Introduction

Despite advances in screening techniques leading to early detection of breast cancer, resistance to tumor therapy is still a major challenge in treatment of this disease, and recurrence rates are very high [1,2]. Drug resistance is broadly classified into two types; 1) *de novo* (intrinsic) drug resistance in patients that do not respond to conventional therapies, and 2) acquired resistance in patients developed during treatment [3]. Intrinsic and acquired therapy resistances are major challenges for the successful treatment of patients, in particular those with triple-negative breast cancer (TNBC) [4]. TNBC is a subtype of epithelial breast cancer that doesn't express estrogen receptor (ER), progesterone receptor (PR) and human epidermal growth factor receptor 2 (HER2) [5]. Only 15-20% of the total population of breast cancers is triple negative, but these are highly aggressive and metastatic. Due to the absence of specific therapeutic targets, treatment strategies against this tumor subtype are severely limited. As a consequence, current treatment of these tumors is restricted to chemotherapy, frequently leading to development of therapy resistance and recurrent disease [6]. Acquired drug resistance of tumor cells can be driven by a plethora of different mechanisms, like increased drug efflux, tumor cell heterogeneity, inactivation of apoptosis, increased DNA repair, angiogenesis, altered metabolism and stress-induced genetic or epigenetic alterations after drug exposure [3,7–11]. Among these mechanisms, the adaptation of cancer cells to different cellular stress conditions (as induced by anti-cancer drugs) play a particularly important role for therapy resistance. A better understanding of the underlying resistance mechanisms are urgently required to identify new targets for treatment in an aim to improve clinical outcomes of TNBC.

Resistance to cell death caused by defects in apoptotic pathways and overexpression of anti-apoptotic proteins is a general hallmark of cancer [12–14]. Pro- and anti-apoptotic members of the Bcl-2 family are key regulators of apoptotic cell death. The Bcl-2 family proteins can be classified into three subfamilies: (i) the pro-apoptotic BH3-only proteins which have only one domain in common, the alpha helical BH3 domain; (ii) the pro-apoptotic Bax-like proteins which contain three such domains (BH1,2,3) and (iii) the anti-apoptotic Bcl-2-like proteins that contain 4 homology domains (BH1-4) and are regularly overexpressed in cancer. Bax and Bak trigger mitochondrial outer membrane permeabilization (MOMP) that is required for the release of pro-apoptotic factors from the mitochondria into the cytosol. This intrinsic apoptosis pathway is kept in check by the pro-survival Bcl-2 family members (Bcl-2, Bcl-xL, Mcl-1, Bcl-w and Bfl-1) [15–17].

The Hsp70 co-chaperone and anti-apoptotic protein BAG3 (also called Bis) is a member of the Bcl-2-associated anthanogene (BAG) protein family. This highly conserved family of co-chaperone interacts with the ATPase domain of heat shock protein 70 (HSP70) through a specific structural domain – the BAG domain [18]. BAG3 regulates several key hallmarks of cancer, including cell survival, cell adhesion, metastasis, angiogenesis and regulation of proteostasis [19,20]. A key mechanism promoting its anti-apoptotic function is represented by BAG3-dependent stabilization of the pro-survival Bcl-2 family members including Bcl-2, Bcl-xL and Mcl-1, thereby supporting the anti-apoptotic function of these proteins [21,22]. BAG3 expression has been reported to be elevated in various tumors including breast cancer, and we could previously show that estrogen receptor α (ERα) regulates a non-canonical type of autophagy that involves the function of BAG3 and provides stress resistance in ERα-expressing breast cancer cells [23].

Here we investigated the cellular mechanisms promoting enhanced chemotherapy resistance in TNBC cells adapted to growth in the presence of the clinically relevant chemotherapeutic agents 5-Flourouracil (5-FU), Doxorubicin (DOX) and Docetaxel (DOC). We demonstrate that increased apoptosis resistance is associated with enhanced cytoprotective autophagy, elevated expression of the oncogenic co-chaperone BAG3, BAG3-dependent stabilization of pro-survival Bcl-2 proteins and induction of EMT-like changes in gene expression. We also show that genetic and pharmacological interference with BAG3 function is capable to resensitize cells to apoptosis, underscoring the relevance of BAG3 as a target to overcome therapy resistance in TNBC.

Materials and Methods

Materials

Staurosporine (STS) was obtained from Alexis Biochemicals (San Diego, CA, USA). KRIBB11 ((N(2)-(1H-indazole-5-yl)-N(6)-methyl-3-nitropyridine-2,6-diamine)) was acquired from Calbiochem (Darmstadt, Germany). Bafilomycin A1 (Baf A1), YM-1 (2-((*Z*)-((*E*)-3-Ethyl-5-(3-methylbenzo[*d*]thiazol-2(3*H*)-ylidene)-4-oxothiazolidin-2-ylidene)methyl)-1-methylpyridin-1-ium chloride), p-HEMA (Poly (2-hydroxyethyl methacrylate)), Doxorubicin hydrochloride (DOX), Docetaxel (DOC), 5-Fluorouracil (5-FU), 3-[4,5-Dimethylthiazol-2-yl]-2,5-diphenyltetrazolium (MTT), ABT-737 and all other chemicals or biochemicals were purchased from Sigma-Aldrich (Munich, Germany).

Cell lines and Culture

The triple negative parental human breast cancer cell lines BT-549 and MDA-MB-468 were obtained from ATCC/LGC Promochem GmbH (Wesel, Germany). The chemoresistant cell lines were established by continuous exposure to increasing concentrations of the respective drugs to the parental cell lines as previously described [24,25] and derived from the Resistant Cancer Cell Line (RCCL) collection (www.kent.ac.uk/stms/cmp/RCCL/RCCLabout.html). 5-Fluorouracil (5-FU) resistant BT-549 and MDA-MB-468 sublines were cultured under continuous presence of 2000 ng/ml of 5-FU and named as BT-549^{r}5-FU^{2000} and MDA-MB-468^{r}5-FU^{2000} respectively, BT-549 and MDA-MB-468 cell lines were adapted to 40 ng/ml and 20 ng/ml of Docetaxel (DOC) and named as BT-549^{r}DOC^{40} and MDA-MB-468^{r}DOC^{20}respectively, whereas Doxorubicin (DOX) resistant BT-549 and MDA-MB-468 cell lines were cultivated under the presence of 20 ng/ml and 200 ng/ml of DOX and named as BT-549^{r}DOX^{20} and MDA-MB-468^{r}DOX^{200} respectively. BT-549 parental and chemoresistant cells were cultured in Iscove modified Dulbecco's medium (IMDM) supplemented with 10% Fetal Calf Serum (FCS), 4 mM L-glutamine, 10*2 IU/ml penicillin and 100 µg/ml streptomycin, whereas MDA-MB-468 parental and chemoresistant cells were grown in Dulbecco's modified Eagle's medium (DMEM) with F-12 Nutrient Mixture (Ham) supplemented with 10% FCS, 4 mM L-glutamine, 20 mM HEPES, 10*2 IU/ml penicillin and 100 µg/ml streptomycin (all: Gibco/Invitrogen, Karlsruhe, Germany) and cultures were maintained in a humidified 37°C and 5% CO_2 incubator.

Lentiviral Transduction

Lentiviral vector stocks specific for BAG3 (SHCLNV-NM_004281; TRCN0000007294; Sigma-Aldrich) and ATG5

(SHCLNG-NM_004849; TRCN0000151474; Sigma-Aldrich) were used for transduction of both the parental and resistant cell lines of BT-549 and MDA-MB-468 breast cancer cells. Five different small hairpins sequences were included to set the target. (SHC002; Sigma-Aldrich), the pLKO.1-puro Non-Mammalian shRNA control plasmid DNA was used as a negative control. Transduction was executed as previously reported [26].

Cell Viability (MTT) Assay

3,000 cells suspended in 100 µl of medium were seeded per well in 96-well-plates and cultured for 24 h before onset of treatment. After completion of the treatment period, 20 µl of MTT (3-(4,5-dimethylthiazol-2-yl)-2,5-diphenyltetrazolium bromide) from 5 mg/ml of stock solution were added into 100 µl of medium in each well, followed by 3 h of incubation in a humidified 37°C and 5% CO_2 incubator. Following 3 h of incubation, the medium containing MTT reagent was discarded, the formazan crystals formed after MTT treatment were solubilized by adding 100 µl of the mixture of isopropanol/1M HCl (24:1) and gently shaken for 30 min in dark condition. Then absorbance was measured at 560 nm using microplate reader (TECAN GENios, Crailsheim, Germany).

Flow Cytometry

For quantitative estimation of cell death, flow cytometry was performed as previously described [26].

SDS-PAGE and Western Blotting

SDS-PAGE and Western blotting were performed as recently reported [27]. After blocking in 5% BSA for 1 h at room temperature, the nitrocellulose membranes were incubated overnight at 4°C with primary antibodies directed against BAG3 (rabbit, 1:5000, Abnova, Heidelberg, Germany), LC3 (rabbit, 1:1000, Thermo Fisher Scientific, Rockford, USA), p62 (mouse, 1:1000, BD Biosciences, USA), GAPDH (mouse, 1:10,000, Calbiochem) and rest were against Bcl-2, Mcl-1, Bcl-xL, HSP70, HSF-1, Bak, Bax, ATG5, Beclin-1, pFAK (Tyr397), FAK, HSP60, E-cadherin and N-cadherin which were purchased from Cell Signaling Technology (Danvers, USA) raised in rabbit and used in the dilution of 1:1000. Following incubation, primary antibodies were detected by using respective secondary antibodies coupled with infrared dyes in green (800 CW) or red (680 RD) (IRDye goat anti-rabbit or anti-mouse from LICOR Biosciences, Bad Homburg, Germany diluted in 1:10,000 in 3% BSA for 1 h at room temperature and the signals were detected using the LI-COR Odyssey Infrared Imager (LI-COR Biosciences, Bad Homburg, Germany).

Confocal Microscopy

Cells seeded on chamber slide were fixed with paraformaldehyde (4% PFA) after completion of the respective treatments and permeabilized with 0.1% Triton X-100. For assessment of Cellular morphology, cells were stained with Texas Red-X phalloidin (ThermoFisher Scientific, Darmstadt, Germany). DAPI (Applichem, Darmstadt, Germany) was used for nuclear staining in all cases. After mounting on microscope slides, cells were finally analyzed using Nikon C1i confocal microscope.

Quantitative Real-Time PCR

Total RNA isolation and quantitative real-time PCR (qPCR) was executed as previously described [28]. The StepOnePlus™ Real-Time PCR System (Life Technologies, Darmstadt, Germany) was used for the detection of fluorescence signal above the threshold (Ct) value followed by normalization of fluorescence intensity of the samples were performed to the amplification value of the control gene TATA box binding protein (TBP). All the primers for qPCR were purchased from Applied Biosystems (Darmstadt, Germany). Following primers were used for qPCR: TaqMan® Gene Expression Assay primer for *BAG3*(Hs00188713_m1), *CDH1* (Hs01023895_m1), *CDH2* (Hs00169953_m1), *SNAI1* (Hs00195591_m1), *SNAI2*(Hs00161904_m1), *TWIST1*(Hs01675818_S1), *TWIST2* (Hs02379973_s1).

poly-HEMA Coating for Suspension Cultures

poly-HEMA (p-HEMA) solution was prepared by suspending 1mg of p-HEMA powder in 1 ml of 95% of ethanol followed by thorough mixing at 50°C and 750 rpm in Thermomixer comfort (Eppendorf) for overnight. Then the homogenized solution was filtered and pipetted into 24 well plates and allowed to dry inside the safety hood for two days with opened lids. Before the cells were seeded, the wells were properly washed with sterile PBS and finally the cells were allowed to remain in suspension condition throughout the experiment.

Invasion (Boyden-Chamber) Assay

Before seeding the cells into the chamber, the matrigel (Corning transwell insert with 8 µm pore, Corning, Tewksbury, MA) was rehydrated with 500 µl of FCS-free medium for 2 hours inside the humidified 37°C and 5% CO_2 incubator. Then approximately 750 µl of medium containing 10% FCS was added into the wells of the 24-well cell culture insert companion plate. After discarding the rehydration medium, the transwell inserts were put into the wells of the cell cultured insert companion plate carefully by avoiding air bubble. Then approximately 20,000 cells suspended in 500 µl medium containing 2% FCS were seeded into the matrigel coated insert. After 20 hours of incubation, the cells on the top of the inserts were removed by using Q-tips and the cells attached to the bottom of the inserts were fixed with methanol for 2 minutes followed by staining for another 2 minutes with 0.1% crystal violate. The chambers were washed three four times in purified water and allowed to air dry. Then 6 pictures of each matrigel were captured with a Nikon TS100 inverted microscope equipped with a charge-coupled device (CCD) camera followed by counting of stained cells by using ImageJ software. Three matrigel chambers were used for each condition and each experiment was repeated 3 times.

Migration (Scratch) Assay

400,000 cells were seeded per well in 6 well cultured plates. After 24 hours of incubation, 10 µg/ml of Mitomycin C (Sigma-Aldrich) was added for 2 hours to prevent cell proliferation. Then a scratch was made using 200 µl pipette tip followed by washing with PBS. Pictures of the scratch at 0 hour time point were taken and the same positions were captured after 20 hours of incubation. The number of cells migrated into the scratch area were counted using ImageJ software. Each experiment was repeated for 3 times.

Subcellular Fractionation

The digitonin-based subcellular fractionation technique was employed for the separation of cytosolic and mitochondrial fractions as previously described [29].

Global Proteomics Analysis

For global proteomic analysis, the cells were grown until ~70% confluency. For each cell line, three independent samples were taken. Samples for LC-MS/MS analysis were prepared according to Kulak *et al.* with minor modifications [30]. In brief, cell lysis and protein denaturation were performed by boiling the samples in 6 M GnHCl, 100 mM Tris pH 8.5, 10 mM TCEP and 40 mM ChlAA. Proteins were digested with Lys-C for 3 hours, followed by tryptic digestion overnight. Tryptic peptides were desalted and concentrated using STAGE-Tips (Empore C18, 3M).

Peptides were separated on an easy nLC 1200 (ThermoFisher Scientific) and a 15 cm long, 75µm ID fused-silica column, which has been packed in house with 1.9 µm C18 particles (Dr. Maisch), and kept at 45°C using an integrated column oven (Sonation). Peptides were eluted by a non-linear gradient from 4% to 48% acetonitrile over 135 minutes and directly sprayed into a QExactive HF mass-spectrometer equipped with a nanoFlex ion source (Thermo-Fisher Scientific). Precursor ions were analyzed with a resolution of 60,000 and the 15 most abundant ions were subjected to HCD fragmentation and resulting fragments were analyzed with a resolution of 15,000. Single charged ions and ions with unassigned charge states were not taken into account for fragmentation and dynamic exclusion was set to 20 s.

Data analysis was done with MaxQuant and essentially default settings [31]. Fragment spectra were searched against the Uniprot human reference proteome (version "December 2017"), with a false discovery rate of 1% on PSM and protein level and at least one unique peptide. Fold changes were determined by LFQ quantification with the "match between runs"-option being activated [32]. Statistical significant changes between parental and resistant cell-lines were determined with Perseus using a Two-sample t-test with a permutation based FDR of 5% and a s0 of 0.6 on log2 transformed LFQ values [33].

The mass spectrometry proteomics data have been deposited to the ProteomeXchange Consortium (http://proteomecentral.proteomexchange.org) via the PRIDE partner repository with the dataset identifier PXD008522 [34]. ProteomeXchange provides globally co-ordinate proteomics data submission and dissemination [34].

Statistics

Data are represented as means ± SEM. For statistical analysis, *t*-test (two-tailed) was applied by using (GraphPad Prism, GraphPad Software, Inc., La Jolla, CA, USA). $p<0.05$ was considered to be statistically significant and was denoted with asterisks or hashtags.

Results

BAG3 is Overexpressed in Chemoresistant Breast Cancer Cells

In our study, the triple negative breast cancer cell line BT-549 was adapted to growth in medium containing either 2000 ng/ml of 5-FU, 40 ng/ml of DOC or 20 ng/ml of DOX; the MDA-MB-468 cell line was similarly adapted to growth in the presence of 2000 ng/ml of 5-FU, 20 ng/ml of DOC or 200 ng/ml of DOX. The 50% inhibitory concentration (IC_{50}) value of each drug was obtained by MTT assays. Table 1 depicts the IC_{50} value of each drug and the level of cross resistance of the BT-549Par (parental control cells), BT-549^{r}5-FU^{2000} (adapted to 5-Fluorouracil), BT-549^{r}DOC^{40} (adapted to Docetaxel), BT-549^{r}DOX^{20} (adapted to Doxorubicin), MDA-MB-468Par (parental control cells), MDA-MB-468^{r}5-FU^{2000} (adapted to 5-Fluorouracil), MDA-MB-468^{r}DOC^{20} (adapted to Docetaxel), and MDA-MB-468^{r}DOX^{200} (adapted to Doxorubicin) cell lines to the chemotherapeutic drugs 5-FU, DOC and DOX. All drug-adapted cell lines displayed increased resistance to the other two chemotherapeutic agents at a varying degree. Further we used staurosporine (STS), a well-recognized apoptotic cell death inducer to investigate the possible changes in the general sensitivity to apoptosis in chemoresistant cell lines and analyzed early apoptosis and total cell death by FACS-based Annexin V/PI-staining. FACS data (Figure 1*A*) revealed that all drug-adapted BT-549 and MDA-MB-468 cell lines are significantly more resistant to STS compared to their parental counterparts, indicating decreased apoptosis sensitivity. Expression analysis of anti-apoptotic and pro-apoptotic Bcl-2 family members by western blot unveiled a prominent increase of Bcl-2, Bcl-xL and Mcl-1 proteins in BT-549^{r}DOX^{20} and MDA-MB-468^{r}5-FU^{2000} cells whereas Bak and Bax expression is decreased in almost all the resistant cells compared to their parental controls (Figure 1*B*). Since we found an increased expression of anti-apoptotic Bcl-2 family proteins in chemoresistant BT-549^{r}DOX^{20} and MDA-MB-468^{r}5-FU^{2000} cells, we also treated these cells with the selective BH3-mimetic ABT-737 to determine whether the drug resistant cells are sensitive to inhibition of Bcl-2 and Bcl-xL. Interestingly, our cell viability assay indicates that both the resistant lines are sensitive to ABT-737, with an increased sensitivity of MDA-MB-468^{r}5-FU^{2000} cells in comparison to control cells (Figure S1). Further, we investigated the expression

Table 1. Establishment of Breast Cancer Cellular Resistant Models

IC_{50} ± SEM	BT-549			
	Par	^{r}5-FU	^{r}DOC	^{r}DOX
5-Fluorouracil (µg/ml)	0.63 ± 0.21	5.89 ± 0.47	4.24 ± 1.39	3.37 ± 0.13
Docetaxel (ng/ml)	8.12 ± 0.84	12.82 ± 1.67	212.56 ± 1.20	37.09 ± 2.18
Doxorubicin (ng/ml)	9.46 ± 1.62	15.97 ± 1.26	180.6 ± 2.09	84.38 ± 1.92
IC_{50} ± SEM	MDA-MB-468			
	Par	^{r}5-FU	^{r}DOC	^{r}DOX
5-Fluorouracil (µg/ml)	1.16 ± 0.14	18.97 ± 0.29	5.97 ± 0.07	4.28 ± 0.83
Docetaxel (ng/ml)	9.74 ± 1.02	12. 62 ± 0.86	63.07 ± 1.93	13.47 ± 0.32
Doxorubicin (ng/ml)	116 ± 1.69	129.20 ± 1.95	338.47 ± 1.40	536.47 ± 1.79

Breast cancer cell line BT-549 was adapted to grow isolatedly with 2000 ng/ml of 5-FU, 40 ng/ml of DOC and 20 ng/ml of DOX; MDA-MB-468 cell line was grown similarly with 2000 ng/ml of 5-FU, 20 ng/ml of DOC and 200 ng/ml of DOX. Then 50% inhibitory concentration (IC_{50}) value of each drug was determined by MTT assay. The values are means of three independent experiments performed in triplicate ± SEM. p values<0.05 were considered to be statistically significant.

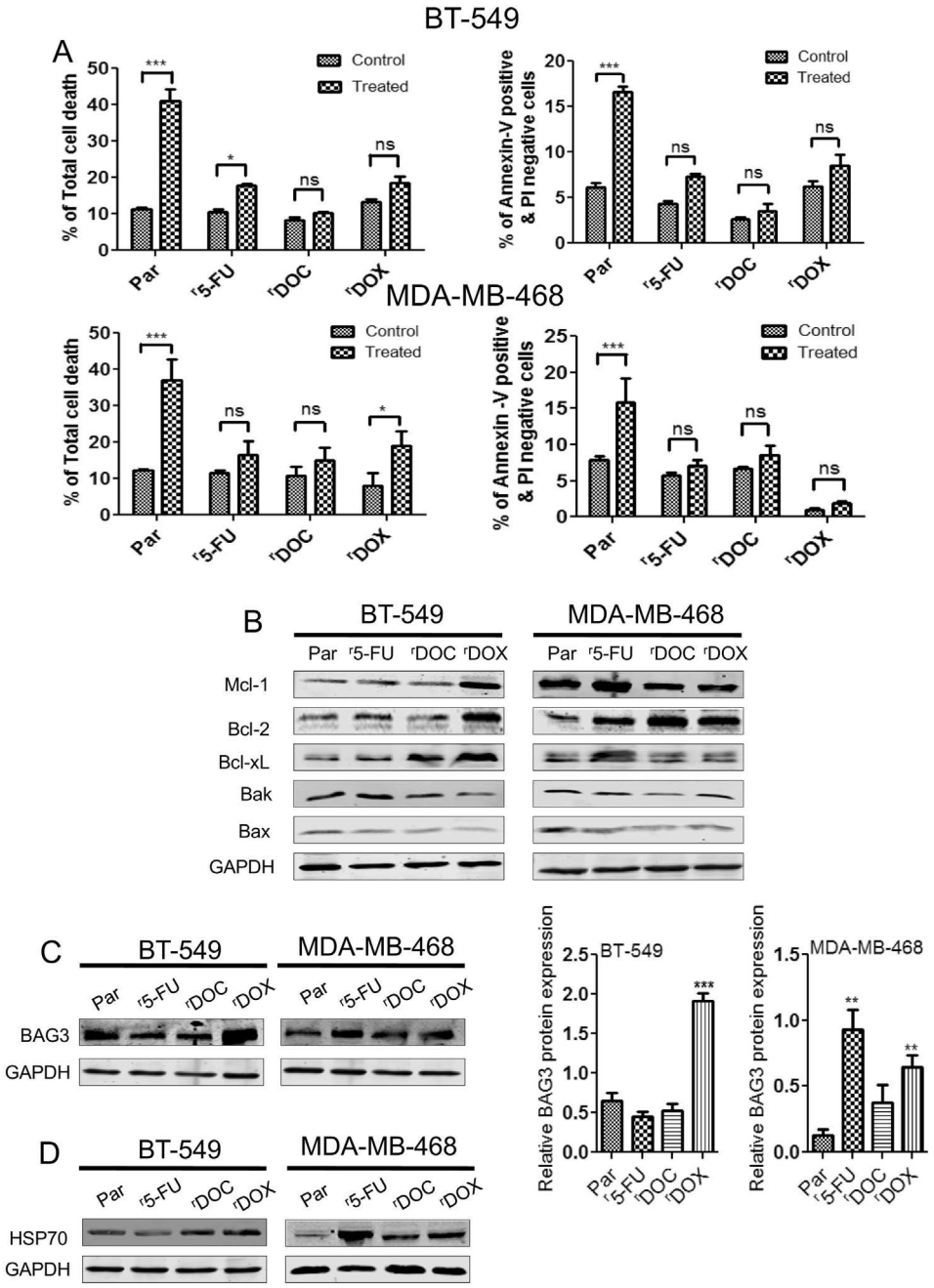

Figure 1. Overexpression of BAG3, HSP70 and other anti-apoptotic proteins and down-regulation of pro-apoptotic proteins in chemoresistant breast cancer cells. (A) BT-549 and MDA-MB-468 parental and chemoresistant cell lines were treated with 3 μM of apoptotic cell death inducer staurosporine (STS) and DMSO (0.1%) as control for 6 hours followed by % of total cell death and % of Annexin-V positive & PI negative cells were estimated by flow cytometry. Data are representative of three independent experiments performed in triplicate. Columns represent means ± SEM. Statistical significance; *p<0.05, ** p<0.01, *** p<0.001 and ns not significant compared to controls (DMSO). (B) Western blot analysis shows anti-apoptotic proteins (Bcl-2, Bcl-xL, and Mcl-1) are over expressed and pro-apoptotic proteins (Bax and Bak) are down regulated in chemoresistant cell lines compared to the parental counterparts. (C) BAG3 and (D) HSP70 are highly expressed in various chemoresistant cell lines. GAPDH was used as loading control. Densitometric analysis of relative BAG3 protein expression was performed in BT-549 and MDA-MB-468 parental and chemoresistant cell lines. Columns represent means ± SEM. Statistical significance; ** p<0.01, *** p<0.001 compared to parental control cells.

levels of HSP70 and BAG3, a HSP70 co-chaperone in all the parental and chemoresistant cells. Western blot analysis revealed a pronounced increase of BAG3 and HSP70 in most of the chemoresistant cell lines, with BT-549^{r}DOX^{20} (Figure 1*C*) and MDA-MB-468^{r}5-FU^{2000} (Figure 1*D*) cells showing the highest expression compared to their parental control cells, respectively.

Attenuation of Autophagy Increases the Sensitivity of Chemoresistant Breast Cancer Cells

One of the potential mechanisms contributing to cell survival in chemoresistance is increased autophagy [35]. To further investigate this possibility in our cell models, we explored the basal autophagy status in all the parental and chemoresistant cells as a starting point.

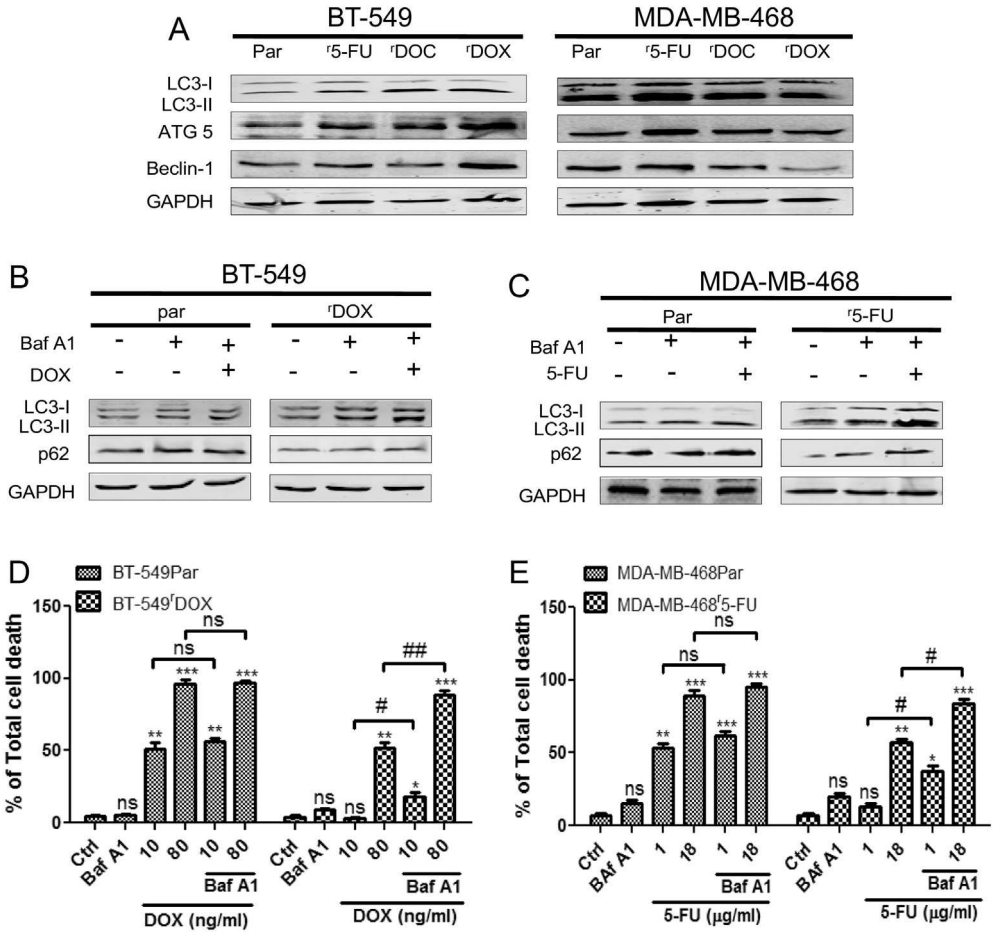

Figure 2. Induction of prosurvival autophagy in chemoresistant cells and pharmacological inhibition of autophagy augments the sensitivity of chemoresistant breast cancer cells (A) Basal level of autophagy was increased in chemoresistant cells as LC3-II, ATG5 and Beclin-1 proteins expression were increased in chemoresistant cells compared to their respective parental cells in western blot analysis. (B) Autophagic flux was determined by the accumulation of LC3-II and p62 after combined treatment of DOX (10 ng/ml) for 72 h and autophagic flux inhibitor Baf A1 (25 nM) for 4 h in both the BT-549Par and BT-549^{r}DOX^{20} cells and (C) similarly in MDA-MB-468Par and MDA-MB-468^{r}5-FU^{2000} cell lines after combined treatment of 5-FU (1 μg/ml) for 72 h and Baf A1 (25 nM) for 4 h. GAPDH was used as loading control. (D) Breast cancer cell lines BT-549Par and BT-549^{r}DOX^{20} were treated with 10 ng/ml and 80 ng/ml of DOX for 72 h with or without Baf A1 (25 nM for 4 h), (E) similarly MDA-MB-468Par and MDA-MB-468^{r}5-FU^{2000} cell lines were treated with 1 μg/ml and 18 μg/ml of 5-FU for 72 h with or without Baf A1 (25 nM for 4 h). Total cell death was quantified by Annexin V/PI double staining followed by flow cytometry. Columns represent means of three independent experiments performed in triplicate ± SEM. Statistical significance: * $p<0.05$, ** $p<0.01$, *** $p<0.001$ and ns not significant compared to respective controls (Ctrls); # $p<0.05$, ## $p<0.01$ and ns not significant with Baf A1 treatment compared to without Baf A1 treatment.

Most of the chemoresistant cells exhibited slightly enhanced levels of autophagy marker proteins like LC3-II, ATG5 and Beclin-1 compared to their parental controls, with the most pronounced changes observed in BT-549^{r}DOX^{20} and MDA-MB-468^{r}5-FU^{2000} cells (Figure 2*A*) that were chosen for a subsequent, more detailed analysis. Western blot analysis revealed a shift from LC3-I to LC3-II and accumulation of p62 after combined treatment with Bafilomycin A1 and the respective drugs, i.e. DOX in BT-549Par and BT-549^{r}DOX^{20} cells (Figure 2*B*), and 5-FU in MDA-MB-468Par and MDA-MB-468^{r}5-FU^{2000} cells (Figure 2*C*). The LC3 shift and accumulation of p62 appeared to be more prevalent in the chemoresistant cells, suggesting that the autophagic flux may be increased in these cells compared to parental controls. The effect of autophagy is highly context-dependent and it can promote either cell survival or cell death [36]. In order to evaluate the death-modulating role of autophagy in our chemoresistant cells, a combined treatment of Bafilomycin A1 and the chemotherapeutic drugs was performed. BT-549 cells were treated with 10 ng/ml of DOX (approximate IC_{50} of BT-549Par) and 80 ng/ml of DOX (approximate IC_{50} of BT-549^{r}DOX^{20}), MDA-MB-468 cells were treated with 1 μg/ml of 5-FU (approximate IC_{50} of MDA-MB-468Par), and 18 μg/ml of 5-FU (approximate IC_{50} of MDA-MB-468^{r}5-FU^{2000}) (see Table 1). Then total cell death was assessed by FACS analysis. FACS data revealed a significant increase of total cell death in BT-549^{r}DOX^{20} (Figure 2*D*) and MDA-MB-468^{r}5-FU^{2000} cells (Figure 2*E*) after combined treatment with chemotherapeutics and Bafilomycin A1, whereas the amount of cell death in parental cells remained largely unaltered. We also genetically inhibited autophagy by a stable lentiviral ATG5 knockdown (ATG5 KD). ATG5 is a key molecule in the early stage of autophagosome formation [37] and depletion of ATG5 is an efficient way to interfere with induction of macroautophagy. Stable ATG5 knockdowns were established both in the BT-549par and BT-549

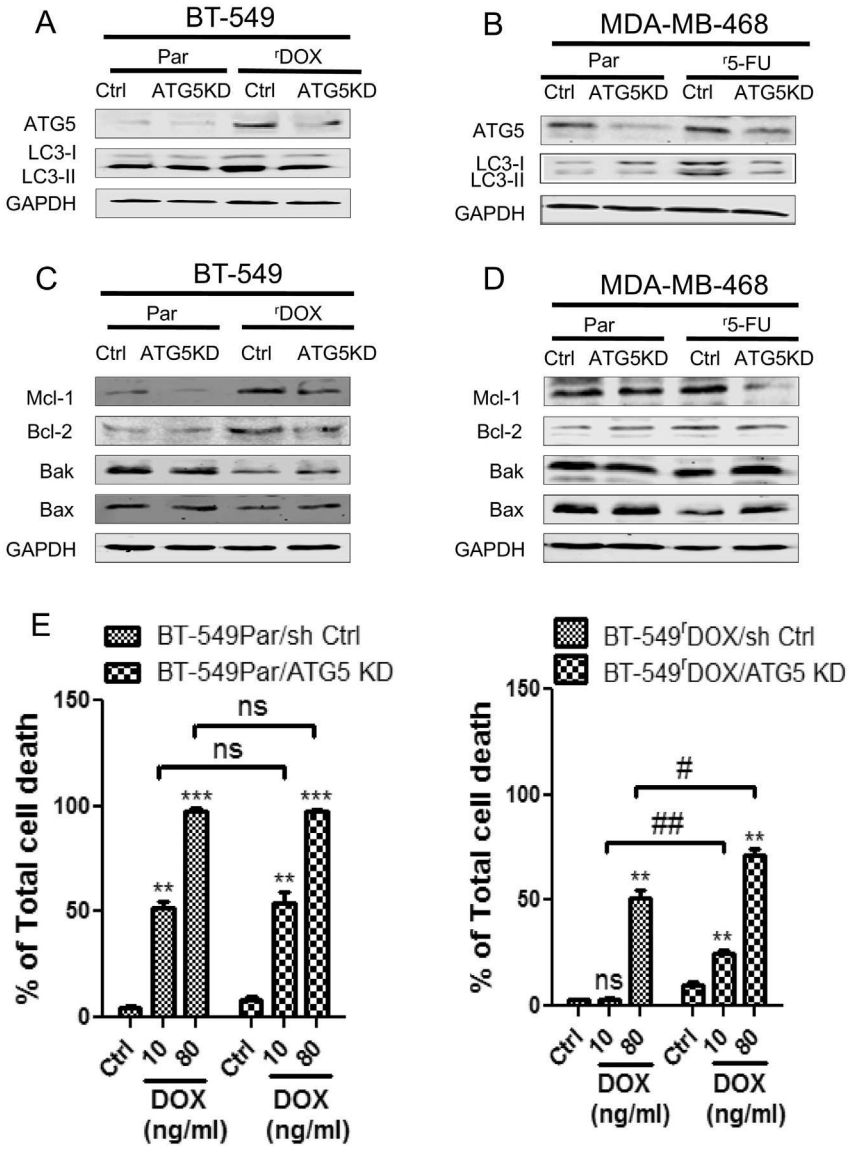

Figure 3. Knockdown of ATG5 sensitizes chemoresistant breast cancer cells (A) Stable lentiviral knockdowns of ATG5 were established in both the BT-549Par and BT-549^{r}DOX^{20} cells and (B) also in the MDA-MB-468Par and MDA-MB-468^{r}5-FU^{2000} cells. Stable lentiviral transduction of control vector was used as control (Ctrl). Knockdowns were confirmed by western blot. Knockdown of ATG5 reduced LC3-II protein expression in BT-549^{r}DOX^{20} and MDA-MB-468^{r}5-FU^{2000} cells. GAPDH was used as loading control in western blot. (C) Down regulation of ATG5 reduces the protein expression of Mcl-1 and other anti-apoptotic proteins, whereas augments the expression of pro-apoptotic proteins likes Bak and Bax in BT-549^{r}DOX^{20}and (D) MDA-MB-468^{r}5-FU^{2000} cells respectively. GAPDH served as loading control in western blot. (E) BT-549^{r}DOX^{20}/ATG5 KD cell exhibited significantly higher levels of total cell death compared to the BT-549Par cells after 72 hours of DOX treatment in a dose dependent manner. 0.1% DMSO for 72 h was used as control. Cell death was determined by Annexin V/PI double staining followed by flow cytometry. Data are means ± SEM of three different experiments each performed in triplicate. * $p<0.05$ ** $p<0.01$, *** $p<0.001$ and ns not significant compared to respective controls (Ctrls); # $p<0.05$, ## $p<0.01$ and ns not significant of ATG5 KD compared to respective sh Ctrls.

^{r}DOX^{20} cells (Figure 3*A*), as well as in MDA-MB-468Par and MDA-MB-468^{r}5-FU^{2000} cells (Figure 3*B*). Knockdown of ATG5 decreased the LC3-II level in BT-549^{r}DOX^{20} (Figure 3*A*) and MDA-MB-468^{r}5-FU^{2000} (Figure 3*B*) cells. Further, we found a decrease in the expression of Mcl-1 and Bcl-2 proteins following knockdown of ATG5 in BT-549^{r}DOX^{20}cells (Figure 3*C*) and also in MDA-MB-468^{r}5-FU^{2000} (Figure 3*D*) cells. For assessment of cell death after ATG5 KD, we performed a dose escalation experiment with DOX for 72 h in the BT-549Par/sh Ctrl, BT-549Par/ATG5 KD, BT-549^{r}DOX^{20}/sh Ctrl and BT-549^{r}DOX^{20}/ATG5 KD cells followed by FACS analysis of total cell death. FACS data revealed a minor, but significant increase of total cell death in the BT-549^{r}DOX^{20}/ATG5 KD cells compared to BT-549^{r}DOX^{20}/sh Ctrl, whereas the amount of cell death in BT-549par/ATG5 KD compared to BT-549par/sh Ctrl remained unaltered (Figure 3*E*). These observations confirm our previous results obtained with pharmacological inhibition of autophagy by Bafilomycin A1. Collectively, we conclude that increased autophagy in chemoresistant cells acts in a cytoprotective manner and may partially contribute to enhanced therapy resistance.

Lentiviral Depletion of BAG3 Resensitizes Chemoresistant Breast Cancer Cells to Therapy

So far we had observed that the higher expression of BAG3 protein is associated with simultaneously increased basal levels of autophagy and enhanced apoptosis resistance in BT-549^{r}DOX^{20} and MDA-MB-468^{r}5-FU^{2000} cells compared to their parental counterparts. BAG3 has key functions in regulation of both autophagy and apoptosis. It maintains cellular homeostasis by selective degradation of damaged proteins after recruiting the macroautophagic pathway [38]. Importantly, it also antagonizes activation of the intrinsic apoptosis pathway through stabilization of Bcl-2 proteins [22]. To further delineate the role of BAG3 as a resistance factor in chemoresistant cells, we established stable lentiviral BAG3 knockdowns in the BT-549Par and BT-549^{r}DOX^{20} cells (Figure 4*A*), and in MDA-MB-468Par and MDA-MB-468^{r}5-FU^{2000} cells (Figure 4*B*), confirmed by western blot and qPCR in BT-549Par and BT-549^{r}DOX^{20} (Figure 4*C*), as well as MDA-MB-468Par and MDA-MB-468^{r}5-FU^{2000} (Figure 4*D*) cells. The level of LC3-II was significantly decreased in the BT-549^{r}DOX^{20}/BAG3 KD cells (Figure 4*A*) and a similar result was also obtained in MDA-MB-468^{r}5-FU^{2000}/BAG3 KD cells (Figure 4*B*). Our western blot data indicates that HSP70 and the anti-apoptotic proteins Mcl-1, Bcl-2 and Bcl-xL are decreased in BT-549^{r}DOX^{20}/BAG3 KD cells (Figure 4*E*) and MDA-MB-468^{r}5-FU^{2000}/BAG3 KD cells (Figure 4*F*) to levels comparable to those observed in parental control cells. These data suggest that interference with BAG3 is able to effectively counteract the chemoresistance-associated increase of Mcl-1, Bcl-2 and Bcl-xL expression. It was previously proposed that BAG3 may also sequester pro-apoptotic BAX in the cytoplasm and serve to inhibit its mitochondrial translocation in glioblastoma cells [21]. Consistent with this hypothesis, we found that mitochondrial BAX was increased in BAG3-depleted MDA-MB-468^{r}5-FU^{2000}cells (Figure S2). To analyze whether knockdown of BAG3 KD also reactivates the sensitivity of the chemoresistant cells to the respective drugs, we performed cell death assays following DOX treatment in BT-549 cell lines and 5-FU treatment in MDA-MB-468 cell lines, respectively. Indeed, our FACS data reveal that both BT-549^{r}DOX^{20}/BAG3 KD (Figure 4*G*) and MDA-MB-468^{r}5-FU^{2000}/BAG3 KD (Figure 4*H*) cells are significantly resensitized to the respective drugs, which was not observed in parental BAG3 KD cells compared to their controls.

Drug Resensitization by Pharmacological Interference with the HSF1/HSP70/BAG3 Pathway

It was recently reported that BAG3 acts as a critical molecule in HSP70-modulated cancer signaling. Thus, targeting the interaction of these two molecules may represent a promising therapeutic strategy [39]. For selective disruption of the HSP70/BAG3 complex, we used YM-1 according to Colvin *et al.* [39]. YM-1 treatment of BT-549^{r}DOX^{20} cells dramatically reduced Mcl-1 levels in a time-dependent manner (Figure 5*A*). Combined treatment with YM-1 and DOX applied at different concentrations synergized in limiting cell viability in BT-549^{r}DOX^{20} cells, but not in the parental BT-549 cells, as confirmed by MTT assays (Figure 5*B*). Furthermore, combined treatment of YM-1 and DOX significantly increased cell death in BT-549^{r}DOX^{20} cells, as detected by Annexin-V staining followed by FACS analysis (Figure 5*C*). Please note that in this experiment, PI staining could not be performed due to the autofluorescence properties of YM-1. The stress induced transcription factor heat shock factor 1 (HSF-1) acts upstream of HSP70 and its co-chaperone BAG3. Since BAG3/HSP70 interaction stabilizes Mcl-1, inhibition of HSF-1 should lead to rapid degradation of Mcl-1 [22]. To further decipher the importance of the HSF-1/HSP70/BAG3 pathway for cell death resistance, the HSF-1 inhibitor KRIBB11 was used in comparison to the experiments previously executed with knockdown of BAG3. The combined treatment of KRIBB11 and DOX significantly increased apoptosis in BT-549^{r}DOX^{20}/sh Ctrl cells; with overall cell death reaching a very similar extent in comparison to BT-549^{r}DOX^{20}/BAG3 KD cells treated with DOX (Figure 5*D*). The expression of BAG3, HSP70, and Mcl-1 and LC3-II proteins gradually decreased in BT-549^{r}DOX^{20} (Figure 5*E*) and MDA-MB-468^{r}5-FU^{2000} cells (Figure 5*F*) in a dose-dependent manner after 48 h treatment of KRIBB11.

BAG3 Depletion Alters Cell Matrix Adhesion in Chemoresistant Breast Cancer Cells

It was previously reported that BAG3 significantly contributed to maintenance of the cell adhesion properties [40]. To explore the effect of BAG3 knockdown on cell adhesion properties of our drug-resistant cells, we performed F-actin staining by using Texas Red-X phalloidin followed by confocal microscopy. Confocal imaging revealed strong alterations in cell morphology in BT-549^{r}DOX^{20}/BAG3 KD cells (Figure 6*A*), while no obvious morphological changes were found in the BT-549Par/BAG3 KD cells. BT-549^{r}DOX^{20}/BAG3 depleted cells were more rounded and loosely attached, whereas the BAG3-proficient cells were more flattened, bigger in size and tightly attached. Similar results were also obtained in MDA-MB-468^{r}5-FU^{2000}/BAG3 KD cells (Figure 6*B*). Western blot analysis revealed that the increase in FAK phosphorylation at Tyr397 residue in BT-549^{r}DOX^{20}cells (Figure 6*C*) and MDA-MB-468^{r}5-FU^{2000} cells (Figure 6*D*) was reduced after BAG3 knockdown. To further assess the sensitivity of the BT-549^{r}DOX^{20}/BAG3 depleted cells to DOX after matrix detachment, cell adhesion was hindered by coating the cell culture plates with p-HEMA, so that all cells were cultured in suspension. Cell death was enhanced in suspension cultures of BAG3-depleted BT-549^{r}DOX^{20} cells after 72 h DOX treatment whereas no significant changes of cell death were noticed in the BAG3 proficient BT-549^{r}DOX^{20} cells in comparison to controls (Figure 6*E*).

Depletion of BAG3 Reverses EMT-Associated Expression Changes in Chemoresistant Breast Cancer Cells

Recently the role of BAG3 in controlling epithelial-mesenchymal transition (EMT) has come to attention of the scientific community [19]. To further investigate this phenomenon in chemoresistant cells, we performed qPCR to analyze the relative mRNA expression levels of several key genes involved in EMT. qPCR data revealed that *CDH1* (encoding E-cadherin) mRNA expression was strongly increased whereas *CDH2* (encoding N-cadherin) and *SNAI1* (encoding Snail) expression was significantly decreased in BAG3-depleted BT-549^{r}DOX^{20} cells (Figure 7*A*) and MDA-MB-468^{r}5-FU^{2000} cells (Figure 7*B*), consistent with the hypothesis that BAG3 promotes EMT. We also found reduced mRNA expression of genes encoding the transcription factors *SNAI2* (Snail2), *TWIST1* and *TWIST2* in BAG3-depleted BT-549^{r}DOX^{20} (Figure S3*A*) and similarly in MDA-MB-468^{r}5-FU^{2000} cells (Figure S3*B*). We did not find any significant changes in the mRNA expression of the above genes in the parental BAG3-depleted cells compared to their controls, except the increase of *TWIST1* mRNA expression in BAG3-depleted parental MDA-MB-468 cells (Figure S3*B*). To further validate our qPCR data, we performed western blot analysis revealing a strong up-regulation of E-cadherin and down-regulation of N-cadherin in

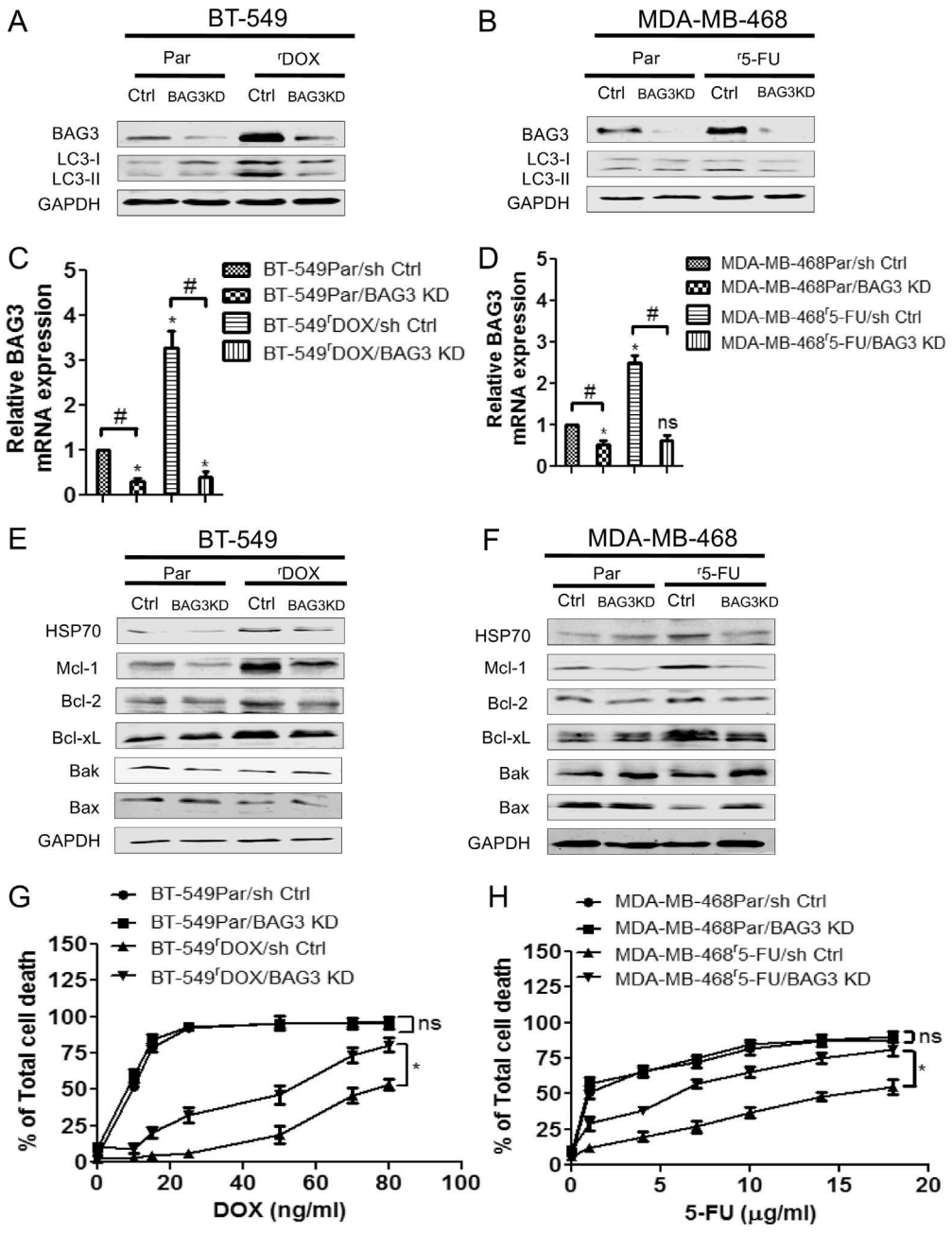

Figure 4. Depletion of BAG3 sensitizes the chemoresistant breast cancer cells by attenuating protective autophagy (A) Stable lentiviral knockdowns of BAG3 were established in both the BT-549-Par and BT-549^{r}DOX^{20} cells and (B) also in the MDA-MB-468Par and MDA-MB-468^{r}5-FU^{2000} cells. Stable lentiviral transduction of empty vector was used as control (Ctrl). Knockdowns were confirmed by western blot. Knockdown of BAG3 reduced LC3-II protein expression in BT-549^{r}DOX^{20} and MDA-MB-468^{r}5-FU^{2000} cells. GAPDH served as loading control in western blot. (C) Relative *BAG3* mRNA expression was also determined by quantitative PCR (qPCR) after stable lentiviral knockdowns of BAG3 in BT-549Par and BT-549^{r}DOX^{20} cell lines and (D) similarly in MDA-MB-468 cells respectively. qPCR data represent means of three independent experiments± SEM (n = 3). Significant *BAG3* mRNA expression compared to parental sh Ctrls are marked by *asterisks*: * p<0.05, ** p<0.01 and ns not significant. Significant differences between BAG3 KD and respective sh Ctrls are denoted by *hashtags*: # p<0.05, ##*p*<0.01 and ns not significant. (E) Knockdown of BAG3 reduced the protein expression of HSP70, Mcl-1 and other anti-apoptotic proteins whereas augments the expression of pro-apoptotic proteins like Bak and Bax in BT-549^{r}DOX^{20} and (F) MDA-MB-468^{r}5-FU^{2000} cells respectively. GAPDH served as loading control. (G) BT-549^{r}DOX^{20}/BAG3 KD and (H) MDA-MB-468-^{r}5-FU^{2000}/BAG3 KD cells exhibited significantly higher levels of total cell death compared to their parental counterparts after 72 hours of DOX and 5-FU treatment in a dose dependent manner respectively. 0.1% DMSO for 72 h was used as control. Cell death was determined by Annexin V/PI double staining followed by flow cytometry. Data represent means of three independent experiments ± SEM (n = 3). **p*<0.05 and ns not significant of BAG3 KD compared to respective sh Ctrls.

BAG3-depleted MDA-MB-468^{r}5-FU^{2000} cells (Figure 7*C*) which corroborated our qPCR data. To investigate whether depletion of BAG3 has any impact on cell invasion and migration properties of the chemoresistant cells, we performed Boyden-chamber assays and scratch assays. BAG3-depleted BT-549^{r}DOX^{20} cells exhibited significantly reduced invasiveness compared to the BAG3-proficient

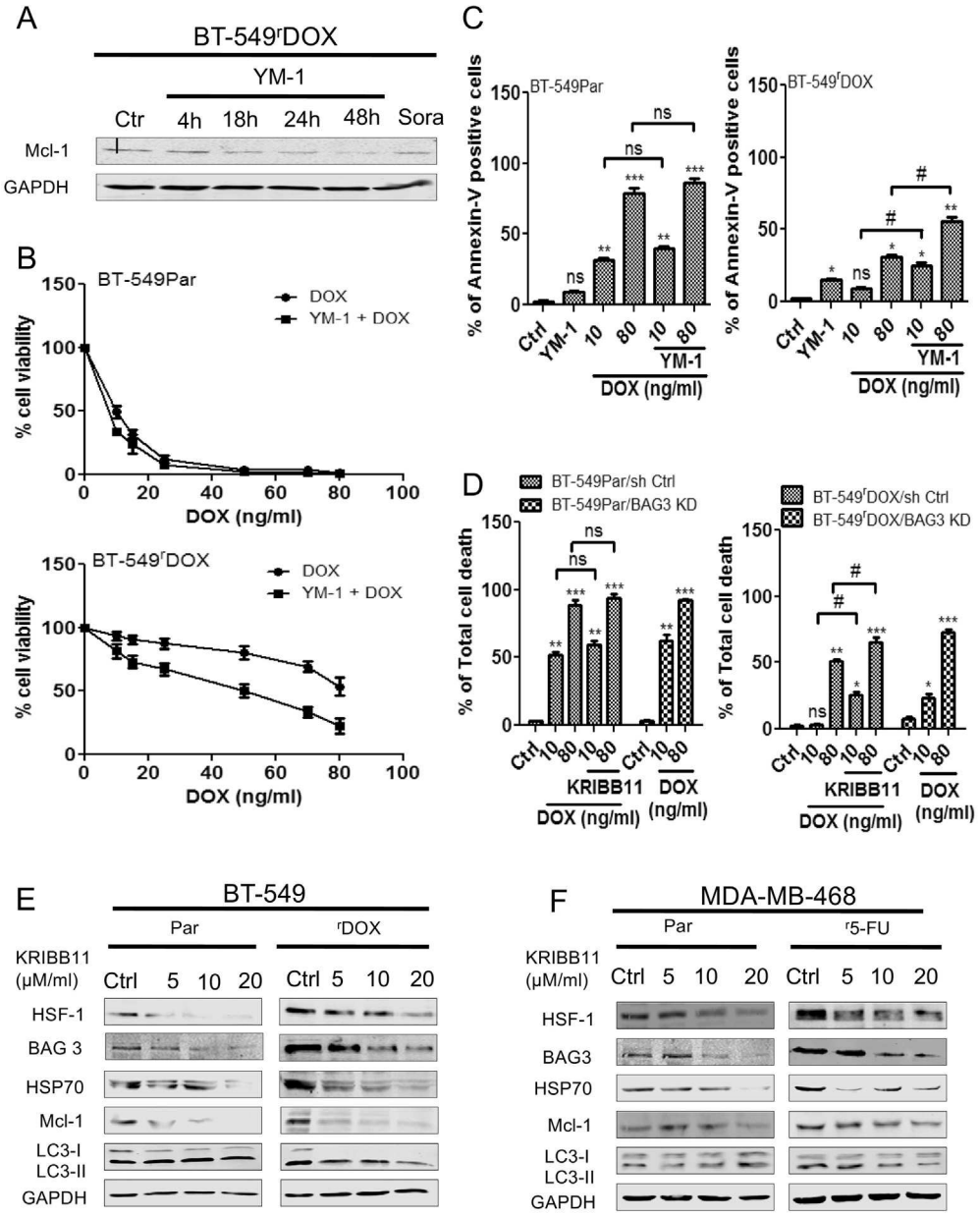

Figure 5. HSP70/BAG3 interaction inhibitor YM-1 and HSF-1 inhibitor KRIBB11 sensitize the chemoresistant breast cancer cells (A) Dissociation of the HSP70/BAG3 complex by YM-1 (5 μM) decreased Mcl-1 expression in BT-549^{r}DOX^{20} cells after 4 h, 18 h, 24 h, 48 h treatment in western blot analysis. 0.1% DMSO for 48 h was used as Control (Ctrl) for the solvent, whereas Sorafenib (Sora) 5 μM for 48 h was used as positive control. GAPDH was used as loading control in western blot. (B) % of cell viability was analyzed by MTT assay in BT-549Par and BT-549^{r}DOX^{20} cells after 2 h pre-treatment of 5 μM of YM-1 for 48 h followed by DOX for 72 h. DMSO 0.1 % for 48 h was used as control (Ctrl) for the solvent. (C) Breast cancer cell lines BT-549Par and BT-549^{r}DOX^{20} were treated with 10 ng/ml and 80 ng/ml of DOX for 72 h with or without YM-1 (5 μM, 48 h). 0.1 % DMSO for 48 h was used as control (Ctrl) for the solvent. Then cell death was analyzed by Annexin-V positive staining in flow cytometry. Columns represent means of three independent experiments ± SEM (n = 3). Statistical significance: * p<0.05, ** p<0.01, *** p<0.001 and ns not significant compared to ctrls (0.1 % DMSO); # p<0.05, ## p<0.01 and ns not significant with combined treatment of YM-1 and DOX compared to DOX treatment alone. (D) Combined treatment of KRIBB11 (20 μM, 48 h) and DOX significantly augment the total cell death in BT-549^{r}DOX^{20}/sh Ctrl cells compared to DOX treatment alone. 0.1 % DMSO for 48 h was used as control (Ctrl) for the solvent. Cell death was determined by Annexin V/PI double staining followed by flow cytometry. Columns represent means of three independent experiments ± SEM (n = 3). Statistical significance: * p<0.05, ** p<0.01, *** p<0.001 and ns not significant compared to ctrls (0.1 % DMSO); # p<0.05, ## p<0.01 and ns not significant with combined treatment of KRIBB11 and DOX compared to DOX treatment alone. (E) KRIBB11 treatment decreased BAG3, HSP70, Mcl-1 and LC3 II in a dose dependent manner in BT-549^{r}DOX^{20} and (F) MDA-MB-468-^{r}5-FU^{2000} cells respectively. Cells were treated with 5 μM, 10 μM and 20 μM of KRIBB11 for 48 h. DMSO (0.1 %, 48 h) was used as control (Ctrl). GAPDH served as loading control for western blot.

BT-549^{r}DOX^{20} cells after 20 h of incubation (Figure 7*D*), and similar results were also obtained in MDA-MB-468^{r}5-FU^{2000}/BAG3 KD cells (Figure 7*E*). Our scratch assays also revealed a significantly reduced motility of BAG3-depleted BT-549^{r}DOX^{20} cells (Figure S4*A*) and MDA-MB-468^{r}5-FU^{2000} cells (Figure S4*B*) after 20 h incubation compared to their controls.

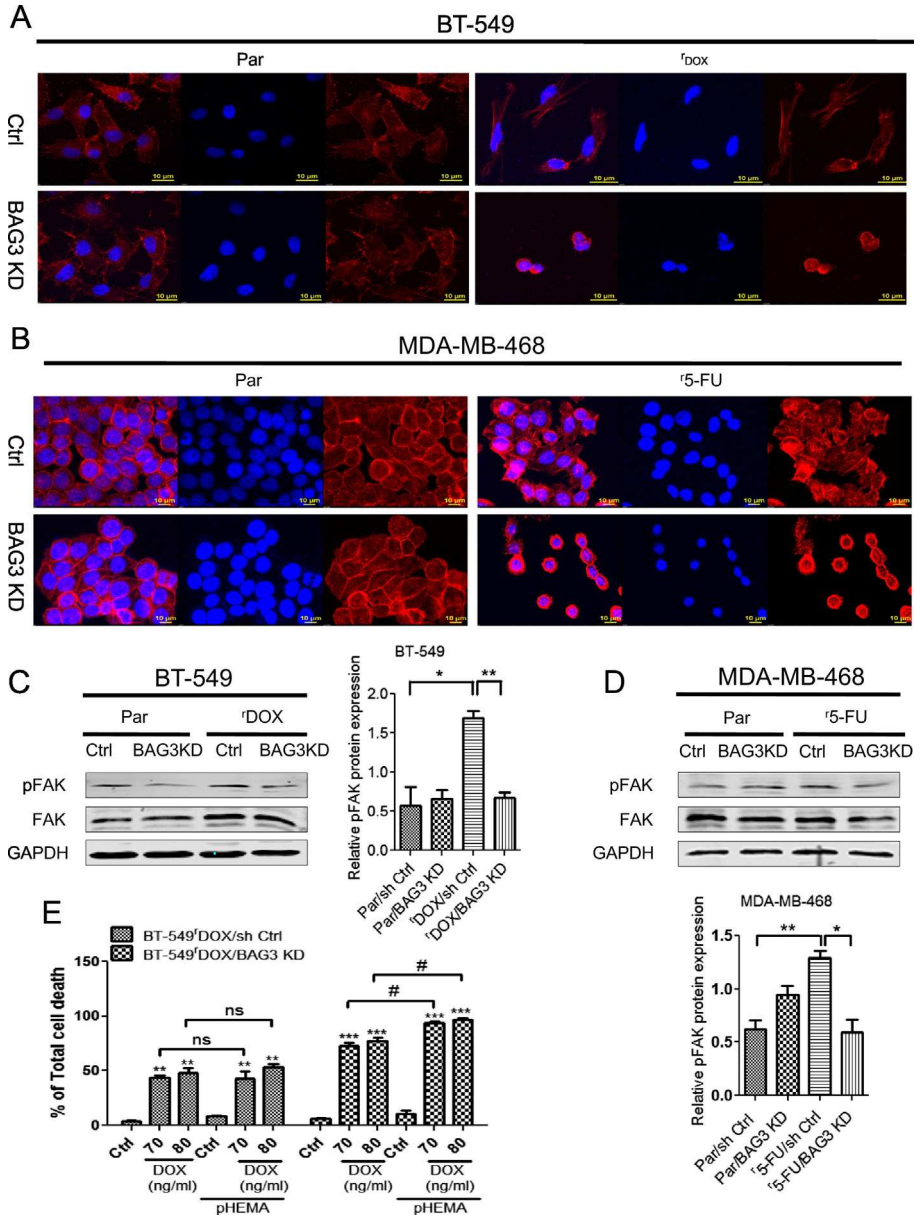

Figure 6. BAG3 depletion alters cell matrix adhesion in chemoresistant breast cancer cells (A) Knockdown of BAG3 altered cellular morphology and actin cytoskeletal distribution in BT-549^{r}DOX^{20} and (B) MDA-MB-468^{r}5-FU^{2000} cells compared to their respective parental counterparts in confocal imaging. For staining of F-actin, Texas Red-X phalloidin was used whereas nuclei were stained with DAPI. Scale bar 10 μm. (C) FAK phosphorylation was reduced in BT-549^{r}DOX^{20}/BAG3 KD and (D) MDA-MB-468^{r}5-FU^{2000}/BAG3 KD cells respectively. GAPDH served as loading control in the western blot. Densitometric analysis of relative pFAK protein expression was performed in control and BAG3 KD of both BT-549 and MDA-MB-468 parental and chemoresistant cell lines. Columns represent means ± SEM. Statistical significance; * $p<0.05$, ** $p<0.01$, *** $p<0.001$ compared to controls (E) BT-549^{r}DOX^{20}/BAG3 KD cells cultured in suspension exhibited more sensitivity to DOX treatment in a dose dependent manner. Cell cultured dishes were coated with pHEMA to prevent cell adhesion. Water (0.1%, 72 h) was used as control (Ctrl) for the solvent. Cell death was determined by Annexin V/PI double staining followed by flow cytometry. Columns represent means of three independent experiments performed in triplicate ± SEM. Statistical significance: * $p<0.05$, ** $p<0.01$, *** $p<0.001$ and ns not significant compared to ctrls (0.1 % water); # $p<0.05$ and ns not significant with combined treatment of DOX and pHEMA compared to DOX treatment alone.

Proteomic Analysis Reveals a Gene Signature Associated with Tumor Aggressiveness

The development of drug resistance is a very complex mechanism including alterations of many different processes and proteins. Thus, we performed global proteomic analysis of BT-549^{r}DOX^{20} compared to BT-549Par using label-free quantification. This analysis showed that out of the 4906 reproducibly quantified proteins groups, 271 and 307 were significantly under- and overrepresented in BT-549^{r}DOX^{20} compared to BT-549Par cells (Figure 8*A*), respectively. The 5 most increased and decreased proteins are also depicted in Figure

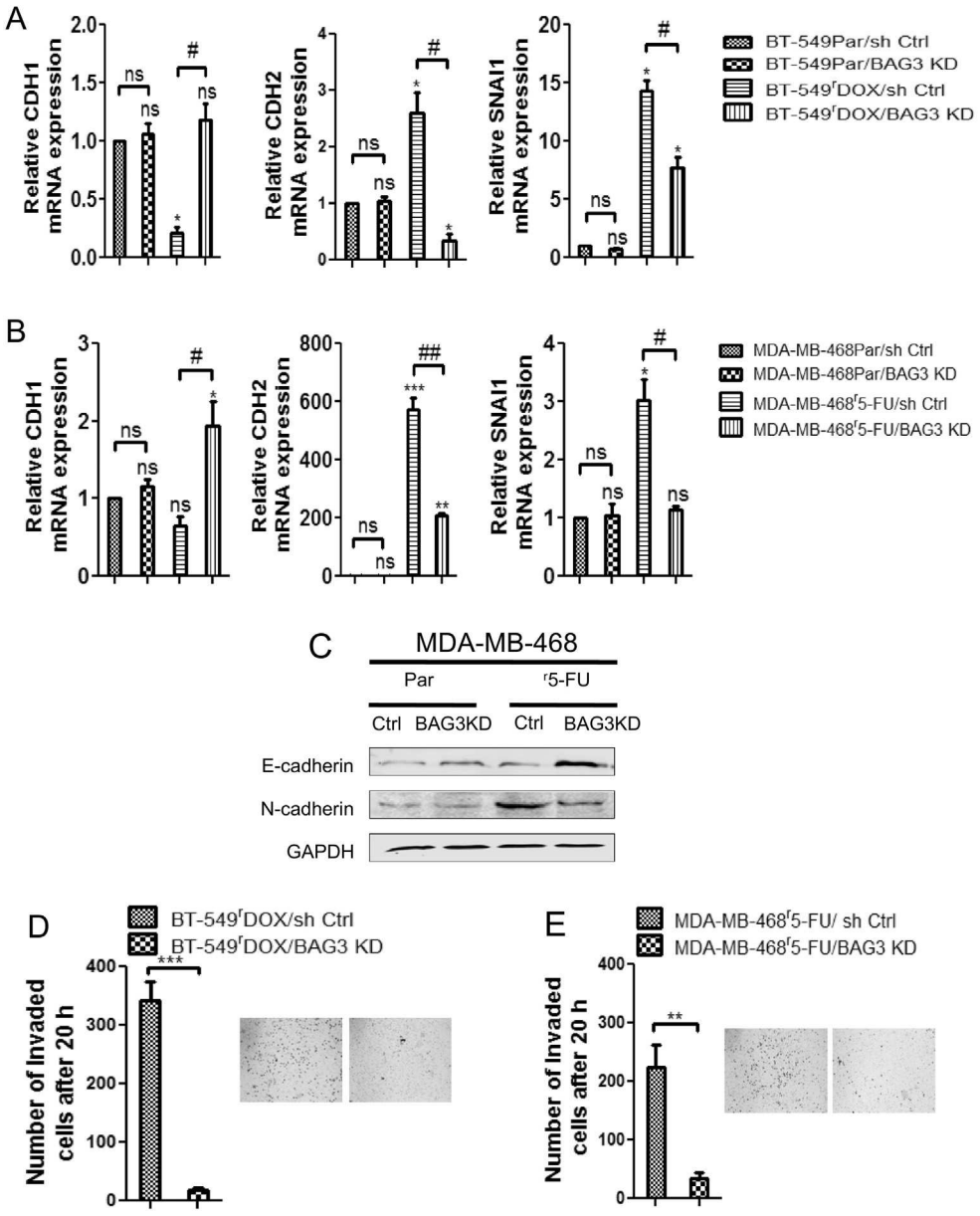

Figure 7. Knockdown of BAG3 reverses the EMT phenomena and simultaneously suppresses invasion in chemoresistant breast cancer cells (A) Knockdown of BAG3 reduced the relative *CDH2*, *SNAI1* mRNA expression, simultaneously increased *CDH1* mRNA expression in BT-549^{r}DOX^{20}/BAG3 KD and (B) MDA-MB-468^{r}5-FU^{2000}/BAG3 KD cells in qPCR respectively. qPCR data represent means of three independent experiments ± SEM (n = 3). Significant mRNA expression compared to parental sh Ctrls are marked by *asterisks*: * $p<0.05$, ** $p<0.01$ and ns not significant. Significant differences between BAG3 KD and respective sh Ctrls are denoted by *hashtags*: # $p<0.05$, ## $p<0.01$ and ns not significant. (C) Expression of E-cadherin protein was increased whereas N-cadherin expression was decreased in MDA-MB-468^{r}5-FU^{2000}/BAG3 KD cells in western blot. GAPDH served as loading control. (D) Number of invaded cells was decreased in BT-549^{r}DOX^{20}/BAG3 KD and (E) MDA-MB-468^{r}5-FU^{2000}/BAG3 KD cells. Invasion assay was performed for 20 h followed by stained with 1% crystal violet, bright field image was taken and invaded cells were counted by using ImageJ software. Columns represent means of three independent experiments ± SEM (n = 3). Statistical significance of invasion: ** $p<0.01$, *** $p<0.001$ and ns not significant with BAG3 KD compared to sh Ctrls.

8*A*, the complete list of significantly changed proteins is provided as a supplemental file (Table S1). Bioinformatics analysis using the freely available STRING-platform (string-db.org); [41] was carried to analyze Gene Ontology (GO) terms that were significantly enriched among the reduced or increased proteins (Figure 8*A*). In total 20 and 27 KEGG pathways were significantly overrepresented among reduced and increased protein groups respectively (Figure 8*B*). Reduced pathways include focal adhesion and cell adhesion molecules (CAMs). Increased pathways include citrate cycle (TCA) and oxidative phosphorylation, two metabolic pathways that are correlated with tumor aggressiveness [42], but also DNA replication and cell cycle, indicating increased proliferation. The analyses of biological processes (GO:BP; Figure 8*C*)

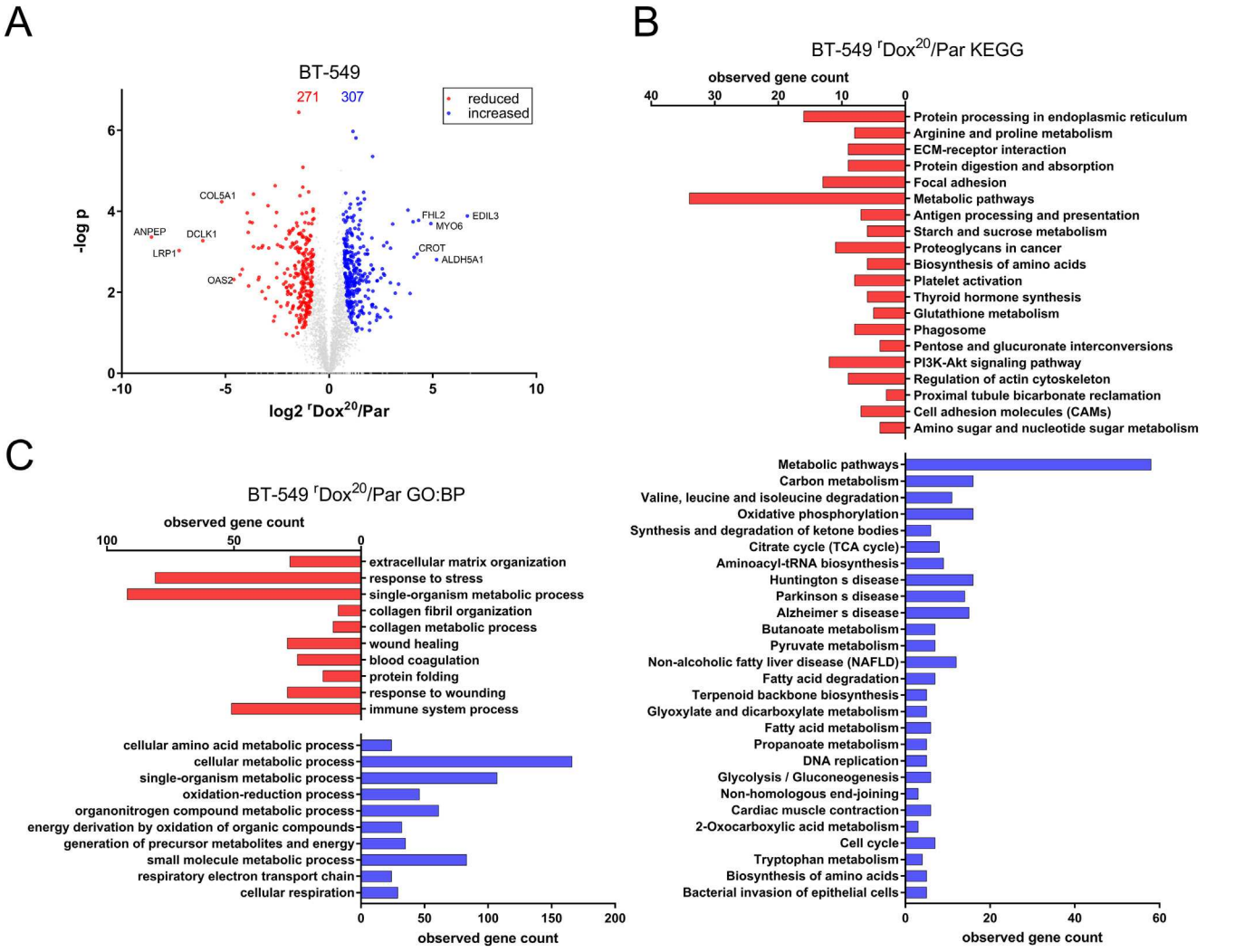

Figure 8. Proteomic analysis reveals a gene signature associated with tumor aggressiveness in BT-549^{r}DOX^{20} cells (A) Volcano-Plot showing the protein ratios (in log2) as a function of the –log p-value of label-free quantification proteomic-data from BT-549^{r}DOX^{20} cells compared to BT-459Par. A total of 4906 proteins were quantified, of those 271 (red dots) and 307 (blue dots) were significantly reduced and increased, respectively. (B and C) Bioinformatic cluster analysis using String (string-db.org; [41]) was performed. (B) Shows all KEGG pathways that are overrepresented among reduced (red) or increased protein groups (blue). (C) Shows the 10 highest ranking Gene Ontology (GO) biological processes (GO:BP) that are overrepresented among proteins with significantly reduced (red) or increased amount (blue).

revealed that among the top 10 processes which were overrepresented among the reduced proteins, extracellular matrix organization (GO.0030198) and response to stress (GO.0006950) are the highest ranking processes. Notably, other processes whose associated proteins were significantly enriched are related to regulation of apoptosis (e.g.: regulation of extrinsic apoptotic signaling pathway (GO.2001236) and regulation of apoptotic signaling pathway (GO.2001233)) and cell adhesion (e.g.: positive regulation of cell adhesion (GO.0045785) and cell-cell adhesion mediated by integrin (GO.0033631)). On the other hand many increased processes are related to an enhanced metabolism, including cellular amino acid metabolic process (GO.0006520), cellular metabolic process (GO.0044237) and also cellular respiration (GO.0045333). Other processes are related to an increased glucose and ATP metabolism (e.g.: gluconeogenesis (GO.0006094), ATP metabolic process (GO.0046034)), replication (DNA strand elongation involved in DNA replication (GO.0006271)). Basically, each of the 10 most increased and decreased single proteins found have previously been related to tumorigenesis or tumor progression (Table 2), thus exemplifying that treatment resistance is accompanied by a more aggressive phenotype.

Discussion

Here we demonstrate that overexpression of BAG3 is associated with chemotherapy resistance of triple negative BT-549 and MDA-MB-468 breast cancer cells that were adapted to growth in the presence of the clinically applied chemotherapeutic agents 5-FU, DOX and DOC. Furthermore, we provide evidence that the increased apoptosis resistance of these cells is associated with BAG3-dependent stabilization of the pro-survival Bcl-2 family proteins Bcl-2, Bcl-xL and Mcl-1, induction of EMT-like transcriptional changes and enhanced cytoprotective autophagy that partially contributes to increased cell survival. In line with our findings, overexpression of BAG3 has been reported in several types of human cancers, such as glioblastoma [21], lung carcinoma [43], pancreatic carcinoma [44],

Table 2. The 10 Highest Ranking Proteins are Listed Along with the NCBI Gene ID, the Log2 Ratio of BT-549^{r}DOX^{20} Over BT-549Par and the –Log P Value, as Well as a Brief Summary of the Known Function of These Proteins in Cancer

Official gene name	Gene-ID	log2 ratio	–log p value	Function
ANPEP	290	-8.567	3.364	Silenced in prostate cancer [53]
LRP1	4035	-7.233	3.030	Cancer cell survival and metastasis [54]
DCLK1	9201	-6.092	3.274	Associated with favorable prognosis in breast cancer [55]
COL5A1	1289	-5.178	4.235	Marker gene for TNBC classification [56]
OAS2	4939	-4.594	2.313	Higher expression in relapsed tumors [57]
STEAP3	55240	-4.294	2.433	Part of a metastasis gene signature [58]
PLA2G4A	5321	-4.190	2.565	Associated with adverse prognosis [59]
ITPR1	3708	-3.948	3.958	Breast cancer susceptibility locus [60] [61]
SERPINB5	5268	-3.900	3.477	Tumor suppressor in breast cancer [62]
DTX3L	151636	-3.881	2.156	Associated with overall survival and autophagy signature [63]

Official gene name	Gene-ID	log2 ratio	–log p value	Known relevance for breast cancer
EDIL3	10085	6.668	3.885	Cell invasion and metastasis [64]
ALDH5A1	7915	5.188	2.805	Stem-like phenotype [65]; detoxifaction [66]
MYO6	4646	4.908	3.694	Oncogenic in breast cancer [67]
FHL2	2274	4.317	3.774	Oncogenesis and tumor progression [68,69]
CROT	54677	4.242	2.945	Correlates with drug resistance [70]
LMCD1	29995	4.101	2.864	Involved in tumor recurrence [71]
GNG11	2791	4.049	3.740	Cell migration and metastasis [72]
KYNU	8942	3.908	1.968	Metastasis [73]
CUX1	1523	3.804	4.027	Migration, invasion and apoptosis-resistance [74,75]
TAGLN	6876	3.349	2.201	Epithelial mesenchymal transition [76]

leukemia [45], and thyroid carcinoma [46], compared with very low basal levels of BAG3 in non-malignant cells [43]. Consistent with the hypothesis that BAG3 may represent a key resistance factor in breast cancer; a very recent study demonstrated that enhanced BAG3 expression correlates with poor patient survival in this tumor entity [47].

All drug-adapted BT-549 and MDA-MB-468 cell lines displayed cross resistance to chemotherapy and the apoptosis inducer STS, indicating an increase in general apoptosis resistance. BAG3 expression was visibly elevated in all three resistant MDA-MB-468 lines and one of the BT-549 lines. To further address the role of BAG3 in cell death resistance, we performed stable lentiviral BAG3 depletion in the BT-549^{r}DOX^{20} and MDA-MB-468^{r}5-FU^{2000} cell lines. Interestingly, BAG3 depletion led to a robust down-regulation of Mcl-1, Bcl-2 and Bcl-xL and apoptosis was efficiently restored exemplifying its crucial role in apoptosis resistance.

The levels of the autophagy markers LC3-II, ATG5 and Beclin-1 were also found to be elevated in BT-549^{r}DOX^{20} and MDA-MB-468^{r}5-FU^{2000} cells. In our chemoresistant cell models, expression of both Bcl-2 and Beclin-1 was elevated simultaneously, suggesting that interaction of Bcl-2 and Beclin-1 may have no significant effect on the regulation of autophagy in these cells. This notion is consistent with previously reported findings pointing to an indirect effect of Bcl-2 on autophagy that is mediated by inhibiting Bak and Bax [48]. Since pro-survival autophagy is a key mechanism underlying drug resistance of cancer cells in many paradigms [35], we investigated the potential contribution of cytoprotective autophagy in chemotherapy resistance. To this end, we applied the pharmacological autophagy inhibitor Baf A1 and established stable lentiviral knockdowns of ATG5 to block the non-selective macroautophagy pathway. In our experiments, treatment with Baf A1 and knockdown of ATG5 significantly increased apoptotic cell death after treatment with DOX and 5-FU in BT-549^{r}DOX^{20} and MDA-MB-468^{r}5-FU^{2000} resistant cells respectively, but not in parental cells, indicating that enhanced autophagy may indeed partially contribute to drug resistance.

In a similar fashion, lentiviral knockdown of BAG3 significantly resensitized both resistant cell lines to drug treatment, indicating that BAG3 overexpression is involved in acquired drug resistance. Interestingly, BAG3 depletion was associated with decreased levels of both LC3-I and LC3-II, indicating that BAG3 overexpression may contribute to enhanced autophagy in the resistant setting. Of note, BAG3 was previously shown to regulate total LC3 levels at the translational level, possibly leading to enhanced basal autophagy [49]. We also found that depletion of BAG3 in chemoresistant cells facilitates the translocation of BAX to mitochondria suggesting that BAG3-dependent sequestration of BAX in the cytoplasmic compartment [21] may contribute to the anti-apoptotic effects of BAG3 in breast cancer chemoresistant cells.

In order to overcome the proposed BAG3-driven resistance, we also pharmacologically targeted the BAG3/HSP70/Mcl-1 signaling axis. The *BAG3* gene is a transcriptional target of the stress-induced transcription factor HSF1. KRIBB11 was found to selectively inhibit the transcriptional activity of HSF1 [50], which is required for expression of both BAG3 and its interactor HSP70. Indeed, we could observe significant synergistic effects on cell death in the combination therapy with KRIBB11 and DOX in the BT-549^{r}DOX^{20} cell line. To further scrutinize these pro-apoptotic effects of BAG3 inhibition, we employed the specific HSP70/BAG3 small molecule inhibitor YM-1 that prevents formation and function of the HSP70-BAG3 module [39]. Inhibition of BAG3 by YM-1 significantly decreased the protein levels of Mcl-1 and was able to mimic the sensitizing effect of BAG3 depletion on apoptosis after combined treatment with DOX in BT-549^{r}DOX^{20} cells. These data underscore the pivotal role of the HSP70 interaction in promoting the anti-apoptotic function of BAG3 and highlight the relevance of this complex as a therapeutic target in breast cancer.

Global proteomic analysis of BT-549^{r}DOX^{20} revealed major changes in several pathways/biological processes implicated in tumorigenesis and tumor progression, including cell adhesion. Besides its anti-apoptotic function, BAG3 was also suggested to support cell adhesion and motility [40], and to mediate resistance to anoikis, a special form of apoptosis induced by matrix detachment [27]. The ability of BAG3 to regulate cell

adhesion was proposed to rely on multiple interactors (e.g. PDZGEF2 and CCN1) of BAG3 through different structural domains in this context [51]. Moreover, BAG3 was implicated in cytoskeleton organization by regulating actin folding via interaction with CCT, a cytosolic chaperonin [52]. The important role of BAG3 in cytoskeleton organization was also observed in this study, as demonstrated by gross re-arrangements of the cytoskeletal structure in BAG3-depleted cells that was visualized by actin staining followed by confocal microscopy. In particular, BAG3 depletion was accompanied with a more rounded and loosely attached cellular morphology. A role of BAG3 in controlling epithelial-mesenchymal transition (EMT) was recently proposed [19]. Indeed, we observed an EMT-like expressional shift in chemotherapy-resistant cells compared to parental controls in our cell models. This shift was associated with increased expression of *CDH2* (N-cadherin), *SNAI1* (Snail1), *SNAI2* (Snail2), *TWIST1* and *TWIST2* and decreased expression of *CDH1* (E-cadherin). Consistent with the proposed function of BAG3 in EMT modulation, BAG3 depletion induced a back shift in the expression pattern of these genes to a more epithelial like state and also reduced the invasiveness and motility in the resistant cell models.

Our findings obtained in established cell lines and their drug-resistant derivatives represent a first step in elucidating specific mechanisms of acquired therapy resistance. These data open the avenue for follow-up investigations in patient-derived cultures and *in vivo* models. Collectively, we demonstrate that BAG3 plays a major role for the cell death resistance of breast cancer cells and their response to chemotherapy, as well as their aggressive growth characteristics. Based on the findings of our study, we propose that by stabilizing anti-apoptotic Bcl-2 family members and promoting EMT-like changes, the HSF1/HSP70/BAG3 pathway may play a pivotal role for therapy resistance of breast cancer. Pharmacological intervention with BAG3 and HSP70 function is an interesting approach for combined therapies aimed at synergistically inducing apoptosis in advanced breast cancer and may aid the design of new strategies aimed at overcoming the resistance to current breast cancer therapy.

Supplementary data to this article can be found online at https://doi.org/10.1016/j.neo.2018.01.001.

Acknowledgements

We would like to thank Gabriele Köpf and Hildegard König for outstanding technical support.

Funding Sources

We would like to thank German Academic Exchange Service (DAAD), Germany and Department of Science and Technology (DST-INSPIRE- IF130677), Govt. of India for providing scholarships. This study was supported by the Deutsche Forschungsgemeinschaft (SFB 1177 on selective autophagy).

Conflict of Interest

The authors declare no conflict of interest

References

[1] Martin HL, Smith L, and Tomlinson DC (2014). Multidrug-resistant breast cancer: current perspectives. *Breast Cancer (Dove Med Press)* **6**, 1–13.
[2] Yardley DA (2013). Drug resistance and the role of combination chemotherapy in improving patient outcomes. *Int J Breast Cancer* **2013**, 137414.
[3] Holohan C, Van Schaeybroeck S, Longley DB, and Johnston PG (2013). Cancer drug resistance: an evolving paradigm. *Nat Rev Cancer* **13**, 714–726.
[4] O'Reilly EA, Gubbins L, Sharma S, Tully R, Guang MH, Weiner-Gorzel K, McCaffrey J, Harrison M, Furlong F, and Kell M, et al (2015). The fate of chemoresistance in triple negative breast cancer (TNBC). *BBA Clin* **3**, 257–275.
[5] Schneider BP, Winer EP, Foulkes WD, Garber J, Perou CM, Richardson A, Sledge GW, and Carey LA (2008). Triple-negative breast cancer: risk factors to potential targets. *Clin Cancer Res* **14**, 8010–8018.
[6] Guestini F, McNamara KM, Ishida T, and Sasano H (2016). Triple negative breast cancer chemosensitivity and chemoresistance: current advances in biomarkers indentification. *Expert Opin Ther Targets* **20**, 705–720.
[7] Coley HM (2008). Mechanisms and strategies to overcome chemotherapy resistance in metastatic breast cancer. *Cancer Treat Rev* **34**, 378–390.
[8] Luqmani YA (2005). Mechanisms of drug resistance in cancer chemotherapy. *Med Princ Pract* **14**(Suppl. 1), 35–48.
[9] Szakacs G, Paterson JK, Ludwig JA, Booth-Genthe C, and Gottesman MM (2006). Targeting multidrug resistance in cancer. *Nat Rev Drug Discov* **5**, 219–234.
[10] Gillet JP and Gottesman MM (2010). Mechanisms of multidrug resistance in cancer. *Methods Mol Biol* **596**, 47–76.
[11] Housman G, Byler S, Heerboth S, Lapinska K, Longacre M, Snyder N, and Sarkar S (2014). Drug resistance in cancer: an overview. *Cancers* **6**, 1769–1792.
[12] Hanahan D and Weinberg RA (2000). The hallmarks of cancer. *Cell* **100**, 57–70.
[13] Hanahan D and Weinberg RA (2011). Hallmarks of cancer: the next generation. *Cell* **144**, 646–674.
[14] Igney FH and Krammer PH (2002). Death and anti-death: tumour resistance to apoptosis. *Nat Rev Cancer* **2**, 277–288.
[15] Delbridge AR and Strasser A (2015). The BCL-2 protein family, BH3-mimetics and cancer therapy. *Cell Death Differ* **22**, 1071–1080.
[16] Hardwick JM and Soane L (2013). Multiple functions of BCL-2 family proteins. *Cold Spring Harb Perspect Biol* **5**.
[17] Zheng JH, Viacava Follis A, Kriwacki RW, and Moldoveanu T (2016). Discoveries and controversies in BCL-2 protein-mediated apoptosis. *FEBS J* **283**, 2690–2700.
[18] Rosati A, Graziano V, De Laurenzi V, Pascale M, and Turco MC (2011). BAG3: a multifaceted protein that regulates major cell pathways. *Cell Death Dis* **2**, e141.
[19] Xiao H, Cheng S, Tong R, Lv Z, Ding C, Du C, Xie H, Zhou L, Wu J, and Zheng S (2014). BAG3 regulates epithelial-mesenchymal transition and angiogenesis in human hepatocellular carcinoma. *Lab Investig* **94**, 252–261.
[20] Sturner E and Behl C (2017). The role of the multifunctional BAG3 protein in cellular protein quality control and in disease. *Front Mol Neurosci* **10**, 177–194.
[21] Festa M, Del Valle L, Khalili K, Franco R, Scognamiglio G, Graziano V, De Laurenzi V, Turco MC, and Rosati A (2011). BAG3 protein is overexpressed in human glioblastoma and is a potential target for therapy. *Am J Pathol* **178**, 2504–2512.
[22] Boiani M, Daniel C, Liu X, Hogarty MD, and Marnett LJ (2013). The stress protein BAG3 stabilizes Mcl-1 protein and promotes survival of cancer cells and resistance to antagonist ABT-737. *J Biol Chem* **288**, 6980–6990.
[23] Felzen V, Hiebel C, Koziollek-Drechsler I, Reissig S, Wolfrum U, Kogel D, Brandts C, Behl C, and Morawe T (2015). Estrogen receptor alpha regulates non-canonical autophagy that provides stress resistance to neuroblastoma and breast cancer cells and involves BAG3 function. *Cell Death Dis* **6**, e1812.
[24] Michaelis M, Agha B, Rothweiler F, Loschmann N, Voges Y, Mittelbronn M, Starzetz T, Harter PN, Abhari BA, and Fulda S, et al (2015). Identification of flubendazole as potential anti-neuroblastoma compound in a large cell line screen. *Sci Rep* **5**, 8202–8210.
[25] Michaelis M, Rothweiler F, Barth S, Cinatl J, van Rikxoort M, Loschmann N, Voges Y, Breitling R, von Deimling A, and Rodel F, et al (2011). Adaptation of cancer cells from different entities to the MDM2 inhibitor nutlin-3 results in the emergence of p53-mutated multi-drug-resistant cancer cells. *Cell Death Dis* **2**, e243.
[26] Antonietti P, Gessler F, Dussmann H, Reimertz C, Mittelbronn M, Prehn JH, and Kogel D (2016). AT-101 simultaneously triggers apoptosis and a cytoprotective type of autophagy irrespective of expression levels and the subcellular localization of Bcl-xL and Bcl-2 in MCF7 cells. *Biochim Biophys Acta* **1863**, 499–509.
[27] Antonietti P, Linder B, Hehlgans S, Mildenberger IC, Burger MC, Fulda S, Steinbach JP, Gessler F, Rodel F, and Mittelbronn M, et al (2017). Interference with the HSF1/HSP70/BAG3 Pathway Primes Glioma Cells to Matrix Detachment and BH3 Mimetic-Induced Apoptosis. *Mol Cancer Ther* **16**, 156–168.
[28] Mohrenz IV, Antonietti P, Pusch S, Capper D, Balss J, Voigt S, Weissert S, Mukrowsky A, Frank J, and Senft C, et al (2013). Isocitrate dehydrogenase 1 mutant R132H sensitizes glioma cells to BCNU-induced oxidative stress and cell death. *Apoptosis* **18**, 1416–1425.
[29] Adrain C, Creagh EM, and Martin SJ (2001). Apoptosis-associated release of Smac/DIABLO from mitochondria requires active caspases and is blocked by Bcl-2. *EMBO J* **20**, 6627–6636.

[30] Kulak NA, Pichler G, Paron I, Nagaraj N, and Mann M (2014). Minimal, encapsulated proteomic-sample processing applied to copy-number estimation in eukaryotic cells. *Nat Methods* **11**, 319–324.

[31] Cox J and Mann M (2008). MaxQuant enables high peptide identification rates, individualized p.p.b.-range mass accuracies and proteome-wide protein quantification. *Nat Biotechnol* **26**, 1367–1372.

[32] Cox J, Hein MY, Luber CA, Paron I, Nagaraj N, and Mann M (2014). Accurate proteome-wide label-free quantification by delayed normalization and maximal peptide ratio extraction, termed MaxLFQ. *Mol Cell Proteomics* **13**, 2513–2526.

[33] Tyanova S, Temu T, Sinitcyn P, Carlson A, Hein MY, Geiger T, Mann M, and Cox J (2016). The Perseus computational platform for comprehensive analysis of (prote)omics data. *Nat Methods* **13**, 731–740.

[34] Vizcaino JA, Deutsch EW, Wang R, Csordas A, Reisinger F, Rios D, Dianes JA, Sun Z, Farrah T, and Bandeira N, et al (2014). ProteomeXchange provides globally coordinated proteomics data submission and dissemination. *Nat Biotechnol* **32**, 223–226.

[35] Sui X, Chen R, Wang Z, Huang Z, Kong N, Zhang M, Han W, Lou F, Yang J, and Zhang Q, et al (2013). Autophagy and chemotherapy resistance: a promising therapeutic target for cancer treatment. *Cell Death Dis* **4**, e838.

[36] Fulda S and Kogel D (2015). Cell death by autophagy: emerging molecular mechanisms and implications for cancer therapy. *Oncogene* **34**, 5105–5113.

[37] Mizushima N, Levine B, Cuervo AM, and Klionsky DJ (2008). Autophagy fights disease through cellular self-digestion. *Nature* **451**, 1069–1075.

[38] Gamerdinger M, Hajieva P, Kaya AM, Wolfrum U, Hartl FU, and Behl C (2009). Protein quality control during aging involves recruitment of the macroautophagy pathway by BAG3. *EMBO J* **28**, 889–901.

[39] Colvin TA, Gabai VL, Gong J, Calderwood SK, Li H, Gummuluru S, Matchuk ON, Smirnova SG, Orlova NV, and Zamulaeva IA, et al (2014). Hsp70-Bag3 interactions regulate cancer-related signaling networks. *Cancer Res* **74**, 4731–4740.

[40] Iwasaki M, Homma S, Hishiya A, Dolezal SJ, Reed JC, and Takayama S (2007). BAG3 regulates motility and adhesion of epithelial cancer cells. *Cancer Res* **67**, 10252–10259.

[41] Szklarczyk D, Franceschini A, Wyder S, Forslund K, Heller D, Huerta-Cepas J, Simonovic M, Roth A, Santos A, and Tsafou KP, et al (2015). STRING v10: protein-protein interaction networks, integrated over the tree of life. *Nucleic Acids Res* **43**, D447–D452.

[42] Solaini G, Sgarbi G, and Baracca A (2011). Oxidative phosphorylation in cancer cells. *Biochim Biophys Acta* **1807**, 534–542.

[43] Chiappetta G, Basile A, Barbieri A, Falco A, Rosati A, Festa M, Pasquinelli R, Califano D, Palma G, and Costanzo R, et al (2014). The anti-apoptotic BAG3 protein is expressed in lung carcinomas and regulates small cell lung carcinoma (SCLC) tumor growth. *Oncotarget* **5**, 6846–6853.

[44] Liao Q, Ozawa F, Friess H, Zimmermann A, Takayama S, Reed JC, Kleeff J, and Buchler MW (2001). The anti-apoptotic protein BAG-3 is overexpressed in pancreatic cancer and induced by heat stress in pancreatic cancer cell lines. *FEBS Lett* **503**, 151–157.

[45] Zhu H, Wu W, Fu Y, Shen W, Miao K, Hong M, Xu W, Young KH, Liu P, and Li J (2014). Overexpressed BAG3 is a potential therapeutic target in chronic lymphocytic leukemia. *Ann Hematol* **93**, 425–435.

[46] Chiappetta G, Ammirante M, Basile A, Rosati A, Festa M, Monaco M, Vuttariello E, Pasquinelli R, Arra C, and Zerilli M, et al (2007). The antiapoptotic protein BAG3 is expressed in thyroid carcinomas and modulates apoptosis mediated by tumor necrosis factor-related apoptosis-inducing ligand. *J Clin Endocrinol Metab* **92**, 1159–1163.

[47] Liu BQ, Zhang S, Li S, An MX, Li C, Yan J, Wang JM, and Wang HQ (2017). BAG3 promotes stem cell-like phenotype in breast cancer by upregulation of CXCR4 via interaction with its transcript. *Cell Death Dis* **8**, e2933.

[48] Lindqvist LM, Heinlein M, Huang DC, and Vaux DL (2014). Prosurvival Bcl-2 family members affect autophagy only indirectly, by inhibiting Bax and Bak. *Proc Natl Acad Sci U S A* **111**, 8512–8517.

[49] Rodriguez AE, Lopez-Crisosto C, Pena-Oyarzun D, Salas D, Parra V, Quiroga C, Morawe T, Chiong M, Behl C, and Lavandero S (2016). BAG3 regulates total MAP1LC3B protein levels through a translational but not transcriptional mechanism. *Autophagy* **12**, 287–296.

[50] Yoon YJ, Kim JA, Shin KD, Shin DS, Han YM, Lee YJ, Lee JS, Kwon BM, and Han DC (2011). KRIBB11 inhibits HSP70 synthesis through inhibition of heat shock factor 1 function by impairing the recruitment of positive transcription elongation factor b to the hsp70 promoter. *J Biol Chem* **286**, 1737–1747.

[51] Iwasaki M, Tanaka R, Hishiya A, Homma S, Reed JC, and Takayama S (2010). BAG3 directly associates with guanine nucleotide exchange factor of Rap1, PDZGEF2, and regulates cell adhesion. *Biochem Biophys Res Commun* **400**, 413–418.

[52] Fontanella B, Birolo L, Infusini G, Cirulli C, Marzullo L, Pucci P, Turco MC, and Tosco A (2010). The co-chaperone BAG3 interacts with the cytosolic chaperonin CCT: new hints for actin folding. *Int J Biochem Cell Biol* **42**, 641–650.

[53] Sorensen KD, Abildgaard MO, Haldrup C, Ulhoi BP, Kristensen H, Strand S, Parker C, Hoyer S, Borre M, and Orntoft TF (2013). Prognostic significance of aberrantly silenced ANPEP expression in prostate cancer. *Br J Cancer* **108**, 420–428.

[54] Montel V, Gaultier A, Lester RD, Campana WM, and Gonias SL (2007). The low-density lipoprotein receptor-related protein regulates cancer cell survival and metastasis development. *Cancer Res* **67**, 9817–9824.

[55] Liu YH, Tsang JY, Ni YB, Hlaing T, Chan SK, Chan KF, Ko CW, Mujtaba SS, and Tse GM (2016). Doublecortin-like kinase 1 expression associates with breast cancer with neuroendocrine differentiation. *Oncotarget* **7**, 1464–1476.

[56] Rody A, Karn T, Liedtke C, Pusztai L, Ruckhaeberle E, Hanker L, Gaetje R, Solbach C, Ahr A, and Metzler D, et al (2011). A clinically relevant gene signature in triple negative and basal-like breast cancer. *Breast Cancer Res* **13**, R97.

[57] Callari M, Musella V, Di Buduo E, Sensi M, Miodini P, Dugo M, Orlandi R, Agresti R, Paolini B, and Carcangiu ML, et al (2014). Subtype-dependent prognostic relevance of an interferon-induced pathway metagene in node-negative breast cancer. *Mol Oncol* **8**, 1278–1289.

[58] Savci-Heijink CD, Halfwerk H, Koster J, and van de Vijver MJ (2016). A novel gene expression signature for bone metastasis in breast carcinomas. *Breast Cancer Res Treat* **156**, 249–259.

[59] Caiazza F, McCarthy NS, Young L, Hill AD, Harvey BJ, and Thomas W (2011). Cytosolic phospholipase A2-alpha expression in breast cancer is associated with EGFR expression and correlates with an adverse prognosis in luminal tumours. *Br J Cancer* **104**, 338–344.

[60] Michailidou K, Hall P, Gonzalez-Neira A, Ghoussaini M, Dennis J, Milne RL, Schmidt MK, Chang-Claude J, Bojesen SE, and Bolla MK, et al (2013). Large-scale genotyping identifies 41 new loci associated with breast cancer risk. *Nat Genet* **45**(353-361), 361.e351–361.e352.

[61] Purrington KS, Slettedahl S, Bolla MK, Michailidou K, Czene K, Nevanlinna H, Bojesen SE, Andrulis IL, Cox A, and Hall P, et al (2014). Genetic variation in mitotic regulatory pathway genes is associated with breast tumor grade. *Hum Mol Genet* **23**, 6034–6046.

[62] Maass N, Nagasaki K, Ziebart M, Mundhenke C, and Jonat W (2002). Expression and regulation of tumor suppressor gene maspin in breast cancer. *Clin Breast Cancer* **3**, 281–287.

[63] Gu Y, Li P, Peng F, Zhang M, Zhang Y, Liang H, Zhao W, Qi L, Wang H, and Wang C, et al (2016). Autophagy-related prognostic signature for breast cancer. *Mol Carcinog* **55**, 292–299.

[64] Lee JE, Moon PG, Cho YE, Kim YB, Kim IS, Park H, and Baek MC (2016). Identification of EDIL3 on extracellular vesicles involved in breast cancer cell invasion. *J Proteome* **131**, 17–28.

[65] Marcato P, Dean CA, Pan D, Araslanova R, Gillis M, Joshi M, Helyer L, Pan L, Leidal A, and Gujar S, et al (2011). Aldehyde dehydrogenase activity of breast cancer stem cells is primarily due to isoform ALDH1A3 and its expression is predictive of metastasis. *Stem Cells* **29**, 32–45.

[66] Tomita H, Tanaka K, Tanaka T, and Hara A (2016). Aldehyde dehydrogenase 1A1 in stem cells and cancer. *Oncotarget* **7**, 11018–11032.

[67] Wang H, Wang B, Zhu W, and Yang Z (2015). Lentivirus-mediated knockdown of myosin vi inhibits cell proliferation of breast cancer cell. *Cancer Biother Radiopharm* **30**, 330–335.

[68] Gabriel B, Fischer DC, Orlowska-Volk M, zur Hausen A, Schule R, Muller JM, and Hasenburg A (2006). Expression of the transcriptional coregulator FHL2 in human breast cancer: a clinicopathologic study. *J Soc Gynecol Investig* **13**, 69–75.

[69] Cao CY, Mok SW, Cheng VW, and Tsui SK (2015). The FHL2 regulation in the transcriptional circuitry of human cancers. *Gene* **572**, 1–7.

[70] Hansen SN, Ehlers NS, Zhu S, Thomsen MB, Nielsen RL, Liu D, Wang G, Hou Y, Zhang X, and Xu X, et al (2016). The stepwise evolution of the exome during acquisition of docetaxel resistance in breast cancer cells. *BMC Genomics* **17**, 442–456.

[71] Chang CY, Lin SC, Su WH, Ho CM, and Jou YS (2012). Somatic LMCD1 mutations promoted cell migration and tumor metastasis in hepatocellular carcinoma. *Oncogene* **31**, 2640–2652.

[72] Chou HL, Yao CT, Su SL, Lee CY, Hu KY, Terng HJ, Shih YW, Chang YT, Lu YF, and Chang CW, et al (2013). Gene expression profiling of breast cancer survivability by pooled cDNA microarray analysis using logistic regression, artificial neural networks and decision trees. *BMC Bioinformatics* **14**, 100–110.

[73] Zhou L, Gao HF, Liu DS, Feng JY, Gao DD, and Xia W (2018). Gene expression profiling of brain metastatic cell from triple negative breast cancer: Understanding the molecular events. *Gene* **640**, 21–27.

[74] Vadnais C, Shooshtarizadeh P, Rajadurai CV, Lesurf R, Hulea L, Davoudi S, Cadieux C, Hallett M, Park M, and Nepveu A (2014). Autocrine activation of the Wnt/beta-catenin pathway by CUX1 and GLIS1 in breast cancers. *Biol Open* **3**, 937–946.

[75] Ripka S, Neesse A, Riedel J, Bug E, Aigner A, Poulsom R, Fulda S, Neoptolemos J, Greenhalf W, and Barth P, et al (2010). CUX1: target of Akt signalling and mediator of resistance to apoptosis in pancreatic cancer. *Gut* **59**, 1101–1110.

[76] Lehmann BD, Bauer JA, Chen X, Sanders ME, Chakravarthy AB, Shyr Y, and Pietenpol JA (2011). Identification of human triple-negative breast cancer subtypes and preclinical models for selection of targeted therapies. *J Clin Invest* **121**, 2750–2767.